

**Tacrine derivatives as potential multifunctional
drugs against Alzheimer's disease-
physicochemical and biological properties**

Rajeshwari

Dissertation to obtain the Master of Science Degree in

Chemistry

Supervisors:

Prof. Maria Amélia Santos Seabra

Prof. Sílvia de Vasconcelos Chaves

September 2017

Acknowledgement

I would like to begin by thanking the people who have made the elaboration of this thesis possible, dedicating their time teachings, support and encouragement, namely Professor Maria Amélia Santos and Professor Sílvia Chaves for accepting to be my research supervisor. It's a great privilege to work under their supervision during my research work of this thesis. I am also thankful to all members of Portuguese research group to make this job possible.

In the lab, a special thanks to Master students Daniel, Gaia, Sara and PhD student Asha for all fun moments and sharing of knowledge, and thanks to Dr. Karam Chand as I have utilized his previous work for further investigation in the present thesis.

Special thanks to friends Ana, Lucia, Joao, for all the relaxed and fun moments they gave me.

Finally, I want to thank my parents and my whole family members for their love, constant motivation, and for always be with me in good and bad moments during this course, really I cannot find words to thank you.

Abstract

Alzheimer's disease (AD) is a multifactorial age-dependent neurodegenerative disorder. The main hallmarks are the low levels of acetylcholine (ACh), responsible for memory loss, and the senile plaques, due to misfolding and aggregation of beta amyloid (A β), although disease progression is also enhanced by oxidative stress and metal (Fe, Cu, Zn) dyshomeostasis. Therefore, as multifunctional anti-AD drug candidates, two new series of tacrine derivatives were developed and evaluated, namely as inhibitors of AChE and self-induced A β aggregation along with the radical scavenging and metal chelation capacity. Compounds TAC-BTA (**RSC-1 to 6**) showed quite good AChE inhibitory capacity in the range of IC₅₀ (0.04-0.27 μ M), moderate self-induced A β aggregation inhibition (27-44%), but poor antioxidant activity. In case of TAC-HP hybrids (**TACHP-9 to 16**), they are good AChE inhibitors with IC₅₀ in the range of (0.64-1.71 μ M); some compounds presented reasonably good radical scavenging capacity, EC₅₀ (**TACHP-10**, 450 μ M; **TACHP-12**, 399 μ M; **TACHP-16**, 483 μ M), but all the compounds had very high potency to inhibit self-induced A β aggregation i.e. in the range of (84-95%). Metal chelation studies, performed for **TACHP-12** by spectrophotometric and potentiometric techniques, showed that the chelating affinity depends on the metal ion (Fe>Cu>Zn), with pM values at the physiological pH (pFe = 21.7, pCu = 10.8, pZn = 6.9) confirming the good chelating capacity of the HP moiety. So, due to their multifunctional ability, both series of tacrine derivatives appear as multi-potent agents, which could be selected for further investigation as drug candidates against AD.

Keywords: Alzheimer's disease, tacrine, AChE inhibitors, self-induced A β -aggregation, antioxidant activity, metal chelation.

Resumo

A doença de Alzheimer (AD) é um distúrbio neurodegenerativo multifatorial dependente da idade. As principais características são os baixos níveis de acetilcolina (ACh), responsáveis pela perda de memória, e as placas senis, devido ao envelhecimento e agregação de beta amiloide (A β), embora a progressão da doença também seja reforçada pelo stresse oxidativo e dishomeostasia de metais (Fe, Cu, Zn). Portanto, como candidatos a medicamentos multifuncionais anti-AD, foram desenvolvidas e avaliadas duas novas séries de derivados de tacrina, nomeadamente como inibidores de AChE e da agregação de A β auto-induzida, juntamente com a capacidade anti-oxidante e de quelação de metais. Os compostos TAC-BTA (**RSC-1 a 6**) apresentaram bastante boa capacidade inibitória de AChE, (IC_{50} = 0,04-0,27 μ M), moderada inibição da agregação auto-induzida de A β (27-44%), mas baixa atividade antioxidante. Os híbridos TAC-HP (**TACHP-9 a 16**) são bons inibidores de AChE (IC_{50} = 0,64-1,71 μ M); alguns compostos apresentaram capacidade anti-oxidant (EC_{50}) razoavelmente boa (**TACHP-10**, 450 μ M, **TACHP-12**, 399 μ M, **TACHP-16**, 483 μ M), mas todos apresentaram uma potência elevada (84-95%) para inibir a agregação de A β auto-induzida. Estudos de quelação de metais, realizados para **TACHP-12** por espectrofotometria e potenciometria, mostraram uma boa capacidade quelante dependente do íon metálico (Fe > Cu > Zn), cujos valores de pM ao pH fisiológico (pFe = 21,7, pCu = 10,8, pZn = 6.9), concordam com o esperado para a unidade HP. Assim, devido à sua capacidade multifuncional, ambas as séries de derivados da tacrina aparecem como agentes multi-potentes, que podem ser selecionados para investigação posterior como candidatos de drogas contra AD.

Palavras-chave: doença de Alzheimer, tacrina, inibidores de AChE, agregação auto-induzida da A β ; actividade antioxidante; agentes quelantes.

Contents

Acknowledgement	i
Abstract	ii
Resumo.....	iii
Index of Tables	vi
Index of Figures.....	vii
Index of schemes	viii
List of Abbreviations and Symbols	ix
1. Introduction.....	1
1.1 Alzheimer's disease	1
1.2 Oxidative stress	2
1.3 Amyloid (A β) aggregation (AD pathogenesis).....	2
1.3.1 Role of metal ions.....	2
1.4 Acetylcholinesterase (AChE).....	3
1.4.1 General structure of TcAChE	3
1.4.2 AChE Inhibitors.....	4
1.5 Moieties used in the hybrids of the present work	6
1.5.1 Benzothiazole	6
1.5.2 Hydroxypyridinone	6
2. Literature review	8
2.1 Tacrine-benzothiazole series	8
2.2 Hydroxypyridone-based anti-neurodegenerative agents	9
3. Aim of present work (Thesis)	12
4. Discussion of results	14
4.1 Molecular modeling	14
4.2 Chemistry	16
4.2.1 Mechanism	18
4.3 Biological studies.....	20
4.3.1 TAC-BTA series.....	20
4.3.2 TACHP series.....	22
4.4 Physicochemical studies	26
4.4.1 Antioxidant activity.....	26
4.4.2 Metal chelation	26
5. Conclusion	32
6. Experimental part	33
6.1 Chemistry	33
6.1.1 General Methods and Materials	33
6.1.2 Experimental Procedure.....	33

6.2 Biological activities	40
6.2.1. Material and equipment	40
6.2.2. Anti-oxidant activity.....	40
6.2.3. Acetylcholinesterase Activity Assay	42
6.2.4 Amyloid beta aggregation assay	43
6.2.5 Transmission Electron Microscopy (TEM).....	44
6.2.6 Potentiometric and spectrophotometric studies	45
6.2.7 Molecular modeling	45
6.2.8 Pharmacokinetic study	46
7. References	47
Appendix	50
Annexure 1.	51
Annexure 2.	51
Annexure 3.	53

Index of Tables

Table 1. Summary of activities of TAC-BTA derivatives (RSC-1 to RSC-6) towards radical scavenging (DPPH), inhibition of AChE and A β ₁₋₄₂ self-aggregation and Predicted pharmacokinetic values for TAC-BTA hybrids.....	21
Table 2. Activities of the TACHP derivatives (TACHP-9 TO TACHP-16) towards radical scavenging (DPPH), inhibition of AChE and A β ₁₋₄₂ aggregation and predicted pharmacokinetic values for TACHP hybrids	25
Table 3. Stepwise protonation constants of TACHP-12, global formation constants ^a of its Fe(III), Cu(II) and Zn(II) complexes ($T = 25.0 \pm 0.1$ °C, $I = 0.1$ M KCl, 20% w/w DMSO/water) and pM ^b values.....	31
Table 4. Solution preparation for antioxidant assay	41
Table 5. Solution preparation for Acetylcholinesterase Activity Assay	43
Table 6. Preparation of solutions for Amyloid beta aggregation inhibition assay	44

Index of Figures

Figure 1. a). Schematic view of the active-site gorge of <i>TcAChE</i> ; b). Schematic description of position of CAS and PAS in active site	4
Figure 2. Docking results for the TAC-BTA hybrids with AChE: superimposition of RSC-3 (yellow) with original ligand (green)	15
Figure 3. Docking results for the TACHP hybrids with AChE: superimposition of TACHP-12 (pink) with original ligand (green).....	16
Figure 4. TEM images of A β -aggregation inhibition experiments performed with samples incubated (37 °C) for 24 h. Experimental conditions: [A β ₄₂] = [CuCl ₂] = 25 μ M; [TACHP-12] = 50 μ M; pH 6.6.	24
Figure 5. Potentiometric titration curves of TACHP-12 (20% w/w DMSO/H ₂ O, I = 0.1 M KCl, T = 25.0 \pm 0.1 °C, C _L = 2 \times 10 ⁻⁴ M); a represents moles of base per mole of ligand.....	28
Figure 6. a)Electronic spectra for the 1:3 Fe(III)/TACHP-12 system (C _L = 2.0 \times 10 ⁻⁴ M, pH 2.42-7.43); b)Species distribution curves for the 1:3 Fe(III)/TACHP-12 system (C _L = 2.0 \times 10 ⁻⁴ M).....	29
Figure 7. Species distribution curves for the 1:2 Cu(II)/TACHP-12 system (C _L = 6.7 \times 10 ⁻⁴ M).....	30
Figure 8. Species distribution curves for the 1:2 Zn(II)/ TACHP-12 system (C _L = 6.7 \times 10 ⁻⁴ M)....	30
Figure 9. Graph for the calculation of % absorbance of ligand (TACHP-9) as EC ₅₀	51
Figure 10. Graph for the calculation of AChE inhibition as IC ₅₀ by respective concentration of inhibitor (RSC-6).	52

Index of schemes

Scheme 1. Acetylcholinesterase catalyzes the hydrolysis of acetylcholine to acetate ion and choline	3
Scheme 2. Representation of AChE inhibitors approved for cure of AD	5
Scheme 3. Moieties used to synthesize the studied hybrids (tacrine, benzothiazole, hydroxypyridinone)	7
Scheme 4. (7a-7e) Rpresentation of tacrine- benzothiazole derivative.	8
Scheme 5. Representation of tacrine–S-allylcysteine–benzothiazole (TAC–SAC–BTA) and tacrine–S-propargylcysteine–benzothiazole (TAC–SPRC–BTA) hybrids.....	9
Scheme 6. Derivatives of hydroxypyridones.....	10
Scheme 7. Representation of tacrine-(hydroxybenzoyl-pyridone) hybrids.	10
Scheme 8. Representation of 3-hydroxy-4-pyridinones derivatives.....	11
Scheme 9. Representation of mono-HP functionalised hybrids.	11
Scheme 10. Representation of general structure of both present studied series; a) Tacrine-methoxyphenylbenzothiazole (n = 2,3 and R ₁ = H, Cl); b) Tacrine- hydroxypyridinones (n = 2,3,4 and R ₁ = H, Cl).....	13
Scheme 11. Reagents and conditions: a) MeOH, NaOH (1.1eq), benzyl chloride, reflux b) Ethanol, Ammonia (28%) reflux; c) anhydrous DMF, K ₂ CO ₃ , ClCH ₂ COOEt; d) MeOH, NaOH, H ₂ O; e) anhydrous DCM, NMM, T3P, RT, 7-8 hrs; f) MeOH, H ₂ , Pd/C.	18
Scheme 12. Mechanism of OH protection.....	19
Scheme 13. Mechanism of Michael type addition reaction.....	19
Scheme 14. Acid – amine coupling mechanism	19
Scheme 15. Representation of derivatives of TAC-BTA.....	22
Scheme 16. Representation of TACHP derivatives.....	25
Scheme 17. Reaction of 2,2-diphenyl-1-picrylhydrazyl (DPPH) radical with hydrogen donating ligand to give 2,2-diphenyl-1-picrylhydrazyl hydrazine (DPPHH).....	41
Scheme 18. Reaction of AChE with substrate AChE to give thiol (R-SH)	42
Scheme 19. Reaction of DTNB with a thiol (R-SH).....	43
Scheme 20. Structure of Thioflavin -T dye.....	44

List of Abbreviations and Symbols

%AA – antioxidant activity;

A β - β -amyloid;

ACh – acetylcholine;

AChE – acetylcholinesterase (enzyme);

AChEI – acetylcholinesterase inhibitors;

AChI – acetylcholine iodide;

AD – Alzheimer's disease;

APP – amyloid precursor protein;

A_{sol} – absorbance of the DPPH solution against the blank solution;

A_{sol} – absorbance of the sample against the blank solution;

BChE – butyrylcholinesterase (enzyme);

¹³C NMR – carbon-13 nuclear magnetic resonance;

°C – Celsius degree;

Caco-2 permeability – capacity of absorption in the intestinal tract to the bloodstream;

CAS – catalytic anionic site;

clog P – calculated partition-coefficient (octanol/water);

CNS – central nervous system;

CTF – C-terminal fragment;

DCC – N,N'-dicyclohexylcarbodiimide;

DCM – dichloromethane;

DMF – dimethylformamide;

DPPH – 2,2-diphenyl-1-picrylhydrazyl;

DTNB – 5,5'-dithiobis-(2-nitrobenzoic acid);

eq – equivalents;

EtOAc – ethyl acetate;

ESI – ionization electrospray;

E327 or Glu327 – glutamate 327;

FDA – Food Drug Administration;

h – hour;

^1H NMR – proton nuclear magnetic resonance;

HEPES – 4-(2-hydroxyethyl)-1-piperazineethanesulfonic acid;

H440 or His440 – histidine 440;

%I – percentage of inhibition of enzyme activity;

IC_{50} – half maximal inhibitory concentration;

log BB – passive blood-brain partitioning;

MeOH – methanol;

min – minute;

mL – milliliter;

μL – micro liter;

mM – mill molar;

μM – micro molar;

μ - percentage of yield;

N – normal;

nM – nanomolar;

NMM – N-methylmorpholine;

NMR – nuclear magnetic resonance;

PDB – Protein Data Bank;

PAS – peripheral anionic site;

Phe – phenylalanine residue;

PNS – peripheral nervous system;

ROS – reactive oxygen species;

s – second;

SD – standard deviation;

τ – tau;

T3P – propylphosphonic anhydride solution;

Tac – tacrine;

TBAI – tetrabutylammonium iodide;

TcAChE – *Torpedo californica* acetylcholinesterase;

THF – tetrahydrofuran;

TLC – thin-layer chromatography;

TMS – tetramethylsilane;

TRIS – tris(hydroxymethyl)aminomethane;

Trp – tryptophan;

Tyr – tyrosine;

UV-Vis – ultraviolet-visible;

v_i – initial velocity in the presence of inhibitor;

v_{control} – initial velocity of the control reaction.

1. Introduction

1.1 Alzheimer's disease

Alzheimer's disease (AD) is a chronic, irreversible and progressive disorder, which is characterized by dementia, cognitive impairment and memory loss and finally to death [1], and also the most common cause of dementia [2]. Although the greatest known risk factor in case of AD is increasing age, i.e. usually the majority of people with AD are 65 and older. But it is not just a disease of old age. In fact, from recent studies, 5% of people with AD have found that younger-onset Alzheimer's usually can appear when someone is in their 40s or 50s. Usually early stages of disease characterized by mild memory loss turn out unfortunately in the late-stage in individuals that lose the ability to carry on a conversation and respond to their environment. Also AD is reported as the sixth leading cause of death in the United States. Patients with AD live an average of eight years after their symptoms become noticeable but survival range may vary from 4 to 20 years, depending on age and other health conditions [3].

In AD brains, total brain size shrinks i.e. the tissue has progressively fewer nerve cells and connections, this sort of change in the brain being also witnessed in other disorders. Patients of AD show plenty of other features such as low levels of acetylcholine (ACh), caused by enzyme cholinesterase which is responsible for the hydrolysis of acetylcholine, misfolding of proteins and associated aggregation processes [4], oxidative stress and free radical formation, and the senile plaques and neurofibrillary tangles as a result from deposition of a beta-amyloid ($A\beta$) peptide [2, 4]. Usually this beta-amyloid ($A\beta$) peptide deposition and neurofibrillary tangles (NFTs) are associated with normal ageing, but also considered as main neuro-pathological lesions in AD. From recent research, this hypothesis of development of the amyloid- β ($A\beta$) cascade of AD pathogenesis by amyloid neuronal toxicity was evidenced by some *in vitro* experimental results [5].

Along with this, there is another factor, reported in recent studies, concerning the presence of transition metal ions, such as iron, copper, aluminum and zinc high concentrations in the brain. These metals are believed to change the normal functioning of brain besides catalyzing the free radical formation reaction in the patient body [6]. Redox-active Fe can mediate β -amyloid toxicity resulting in generation of hydrogen peroxide or hydroxyl radical which is responsible for lipid peroxidation and oxidative stress; also Zn^{2+} and Cu^{2+} were reported to promote $A\beta$ aggregation from some *in vitro* studies [7]. So, the synthetic inhibitor with metal chelating capacity could act as a therapeutic agent to cure AD by lowering down free radical formation and destabilizing the $A\beta$ aggregates.

Nevertheless, cholinesterase inhibitors remain the preferred therapy for early and intermediate AD, although antioxidants may delay disease progression. But from the different studies in the field of AD we come to know the fact that AD is multifactorial in nature, and this multifactorial nature of AD is believed to be the main reason for the absence of an effective treatment [8]. This type of disease successfully tackled through a complex pharmacological approach rather than through a single-target strategy. So inhibition of acetylcholinesterase (AChE), antioxidant capacity i.e. scavenging of the free

radical and the bio-metal chelation along with the plaque formation inhibition, can be used as AD therapeutic methods. Now we will discuss some major factor which contributes toward AD.

1.2 Oxidative stress

Oxidative stress is the base of many physiological and patho-physiological phenomena and it is related with inflammation, carcinogenesis, ageing and much other pathology [9]. Basically, oxidative stress is related with the concept of high intracellular levels of reactive oxygen species (ROS) which later used to become the cause of lipids, proteins and DNA damage [10]. These ROS are by-products of aerobic metabolism, including the superoxide anion (O_2^-), hydrogen peroxide (H_2O_2), and hydroxyl radicals (OH), reported to induce pathology by damaging lipids, proteins, and DNA [10]; in recent research, metabolically generated H_2O_2 emerged as a main cause of redox signaling and oxidative stress in the cell mitochondria [11]. The term oxidative stress usually arises when there is imbalance between defensive mechanism, i.e. antioxidant and free radicals, and reactive metabolites, i.e. oxidants [12]. From reported studies, it is also proved that disturbance in homeostasis of redox-active metal ions in the body results in replacement of other metals from their natural binding sites of proteins. The toxic metal interacts with DNA and leads to oxidative deterioration of biological macromolecules [13].

1.3 Amyloid (A β) aggregation (AD pathogenesis)

Amyloid- β (A β) plaques results in the insoluble amyloid β -peptide (A β) fibrillar aggregate genesis in the brain, which is responsible for oxidative stress, inflammation, and neurodegeneration [14]. On this amyloid accumulation in case of AD, "amyloid hypothesis" states that monomer (A β) peptides containing 39–43 amino acids in length are synthesized by the proteolytic cleavage of the parental amyloid precursor protein (APP) by β -secretases and γ -secretases named enzymes [15]. There are two forms of amyloidogenic A β peptides in AD brains: A β_{1-40} and A β_{1-42} . Among these, A β_{1-42} was found to be more toxic; these peptides aggregate, through hydrophobic interactions, and hydrogen bonding interactions possibly leads to higher order structures i.e. fibrils and it has been also hypothesized that fibrils cause neurodegeneration in AD.

1.3.1 Role of metal ions

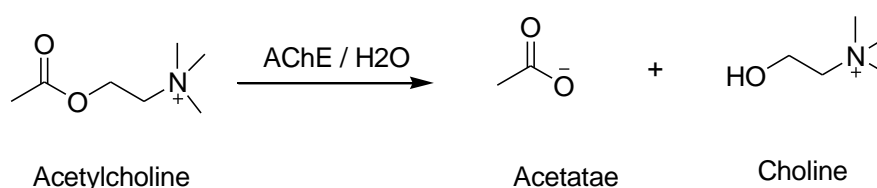
From the many recent researches it has been confirmed that few transition metals, such as Cu, Zn, and Fe, are found in high micro molar to low mili molar concentrations in amyloid plaques and at the synapse. They have high possibility to be involved in the process of generating A β aggregates and their accumulation in the synaptic cleft (e.g. Zn(II)) has ability to aggregate A β into amorphous insoluble aggregates within milliseconds at concentrations $>100 \mu\text{M}$; Cu(II) is responsible for the formation of fibrillar or amorphous aggregates and also accelerates the rate of nucleated aggregate formation as compared to metal-free conditions [16]. Fe(II/III) are redox active metal ions associated with neurotoxicity i.e. oxidative stress [17].

So targeting proteolytic enzymes (β -secretase and γ -secretase) responsible to mediate processing of amyloid precursor protein (APP), and through destruction of existing amyloid deposits

through immunotherapy, which provides enhancement of A β clearance [18] could be effective in the treatment of AD.

1.4 Acetylcholinesterase (AChE)

Acetylcholinesterase (AChE) enzyme is located at the neuromuscular junctions and synaptic cleft, and functions to terminate synaptic transmission by hydrolyzing the neurotransmitter acetylcholine (ACh) into choline and acetic acid (see **Scheme 1**.) AChE is highly specific in its activity, functioning at a rate approaching that of a diffusion-controlled reaction [19].



Scheme 1. Acetylcholinesterase catalyzes the hydrolysis of acetylcholine to acetate ion and choline

1.4.1 General structure of TcAChE

TcAChE is reported as belonging to the class of α/β proteins [19], consisting of a 12-stranded central mixed β -sheet surrounded by 14 α -helices. It has a narrow gorge about 20 Å long, which penetrates more than half-way into the enzyme, and widens out close to its base which contains the active site i.e. lined by 14 aromatic residue rings. The active site consists of S200(Ser), E327(Glu) and H440(His) residues, these three residues forming a planar array; there is also present the oxyanion hole, which would be formed by the amide NH of the following C-terminal residue, A201(Ala) in AChE, and also present S200-O_y, which can be seen looking down the gorge from the surface of the enzyme, being about 4Å above the base of the gorge. The rings of 14 aromatic residues contribute a substantial portion (\approx 40%) of the surface of the gorge; it has been also noticed that the gorge contains only a few acidic residues, which include D285(Asp) and E273(Glu) at the very top, D72, hydrogen-bonded to Y334(Tyr), about half-way down, and E199(Glu), near the base. There is also present tryptophan in the active site of AChE [19, 20] and W84(Trp) was identified as part of the putative 'anionic' (choline) binding site. Apart from this, it possesses two more active sites, catalytic anionic site (CAS) and peripheral anionic site (PAS). Three important amino acids, Phe330, Trp84 and Glu199 forms CAS, which is situated at the lower part of the gorge, while PAS is located at the entrance of the gorge and formed by Trp279, Asp72 and Tyr70, as presented in **Figure 1**.

It was evidenced, in previous studies, that in this deep pocket of the AChE enzyme, acetylcholine (substrate) can slip inside with water molecule and get hydrolyzed into acetic acid and choline. The compounds which have the capability to interact at both CAS and PAS site of the enzyme can fill up this deep pocket and have proved to be good AChE inhibitors.

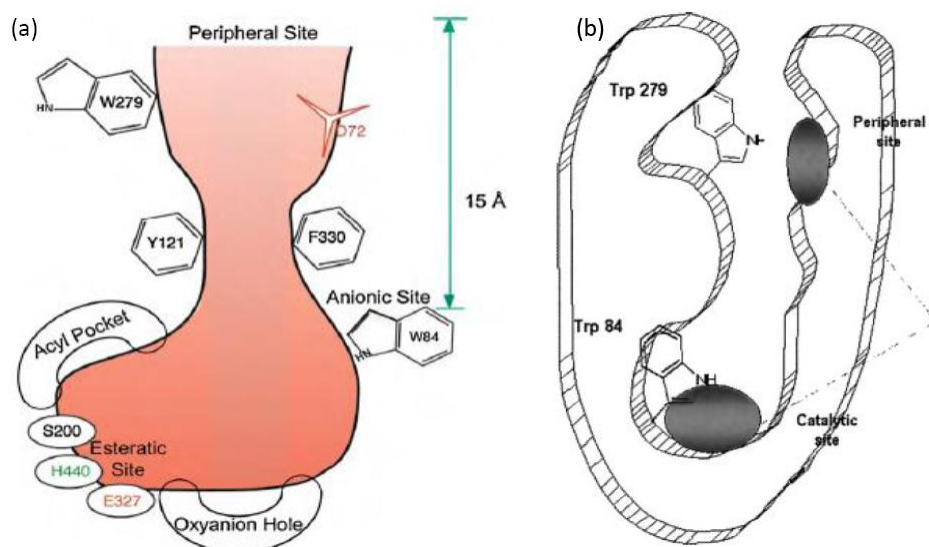


Figure 1. a). Schematic view of the active-site gorge of *TcAChE*; b). Schematic description of position of CAS and PAS in active site. [19]

1.4.2 AChE Inhibitors

Some few anti-AD drugs were approved by regulatory agencies, but four of them were only cholinesterase inhibitors (rivastigmine, donepezil, galantamine, and tacrine) [21] thus capable of reducing AD symptoms by inhibiting AChE, which is responsible for the hydrolysis of ACh at the synaptic cleft. Working of these drugs depends on cholinergic hypothesis, according to which selective loss of cholinergic neurons in case of AD leads to deficiency of ACh in specific areas of the brain which are responsible for learning and memory functions [22].

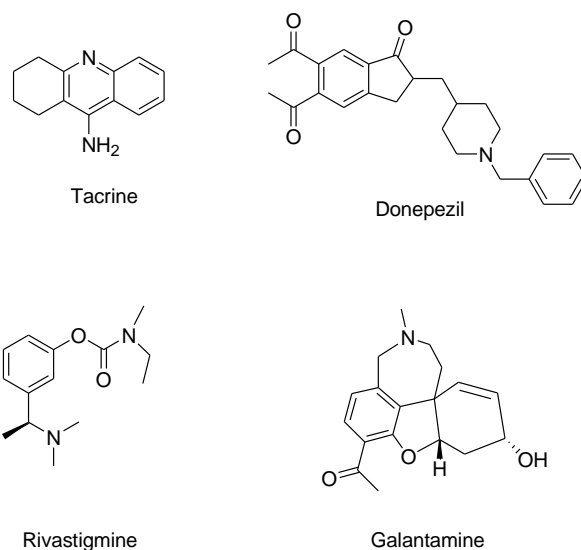
1.4.2.1 Tacrine

Tacrine is the first FDA approved safe and effective drug for the treatment of Alzheimer's disease. Tacrine is a planar three ring acridine i.e. (1,2,3,4-tetrahydro-5-aminoacridine or THA), as shown in **Scheme 2**, It has the ability to slice through cell membranes easily and was approved as anti-AD drug in 1993 [23]. Tacrine THA, 1,2,3,4-tetrahydro-5-aminoacridine, can be administrated orally in the body and in reference to AD it has numerous mechanisms of action, but the putative principle mechanism of action for Alzheimer's disease is as a non-competitive reversible acetylcholinesterase inhibitor [22, 23]. Moreover, tacrine has been concluded to deplete the amyloid deposition in the pathology of this disease, actually blocking the secretion of Beta amyloid precursor protein [24]. Through the clinical pharmacokinetics studies of literature it has been reported that tacrine is rapidly absorbed with a bioavailability 10 to 30%. Tacrine is about 55% bound to plasma proteins and has a clinical half-life of about 3-6 h through a single oral dose [25], and the apparent

volume of distribution is 182 L, with the mean plasma half-life during terminal elimination phase of 2.5. From these studies, it seems that tacrine is uniquely suited to treat AD, although some adverse side effects have been reported, such as nausea, diarrhea, dyspepsia, rhinitis, myalgia, tremor, excessive urination and hepatotoxicity [26].

1.4.2.2. Other AChE inhibitors

Rivastigmine was also approved as a drug for AD in 2000 by the means of oral administration, later on identified with some level of hepatotoxicity [27] and bad for gastrointestinal system [28]. Due to these limitations a new drug was discovered i.e. Donepezil [29], from the investigations Donepezil was found to be good AChE inhibitor ($IC_{50} = 5.7 \text{ nM}$) 1250-fold more selective for butyrylcholinesterase (BuChE, $IC_{50} = 7138 \text{ nM}$), without hepatotoxicity [30], donepezil drug with N-benzylpiperidine and indanone moieties as shown in **Scheme 2**, were concluded to having quite good interaction binding sites with AChE, and are responsible for inhibitory selectivity [31]. Also Galantamine was approved as a drug for the treatment of AD in 2001; it is the most recent one. It is a tertiary alkaloid as shown in **Scheme 2**, with dual mode of action, It is a reversible, competitive AChE inhibitor [28], Galantamine reported with quite good pharmacokinetic characteristics i.e. predictable linear elimination kinetics at the recommended maintenance doses (16 and 24 mg/day), but relatively short half-life (approximately 7 h), and high bioavailability.



Scheme 2. Representation of AChE inhibitors approved for cure of AD

1.5 Moieties used in the hybrids of the present work

The present work is focused on the synthesis of tacrine derivatives (tacrine hybrids) and their evaluation as drugs for Alzheimer's disease treatment through *in vitro* physicochemical (antioxidant activity, metal chelation) and biological analysis, i.e. cholinesterase inhibition assay and beta-amyloid (A β) anti-aggregation peptide assay. These recently designed tacrine derivatives were classified in two series. The first series is composed of tacrine-benzothiazole (TAC-BTA) hybrids, which are based on combination of both TAC and BTA moieties with adequate linkers and substituent groups between both units to improve biological properties. The second series is based on the hybridization of tacrine with a hydroxypyridinone moiety (TACHP), again, using adequate linkers between both main moieties and also substituent groups to improve biological properties. The reason behind choosing these moieties for the synthesis of multifunctional drugs against AD is that they have some role that could be useful in multi-targeting AD. So, in the sections below, these two extra-functional moieties will be described in more detail.

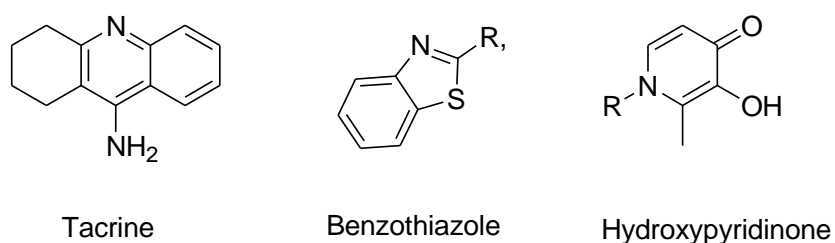
1.5.1 Benzothiazole

The benzothiazole moiety basically represents a heterocyclic system comprising a benzene ring fused with a thiazole ring, containing nitrogen and sulphur in its structure (**Scheme 3**). From the literature research, this kind of heterocyclic fused ring membered compounds were also reported to be present in the many natural molecules i.e. sugar and their derivatives, vitamin C, vitamin B group [32], and so it was also introduced in some synthetic molecules. From the synthetic molecules with benzothiazole moiety many good results have been observed in case of many diseases such as tumour, bacterial infection, tuberculosis, viral infections, and diabetes. Benzothiazole molecules found to be evaluated for as therapeutic drug candidates for the treatment of epilepsy and neurodegenerative diseases such as Alzheimer's disease [33], and many benzothiazole derivatives were also reported as potential β -amyloid imaging probes, i.e. fluorescent tracers for detecting β -amyloid in Alzheimer's brains [34]. Some of the benzothiazole phosphonate derivatives were found to be the antagonistic inhibitor of Amyloid binding alcohol dehydrogenase (ABAD) i.e. mitochondrial enzyme reported to induces dysfunction of mitochondria in synaptic cleft because of the some interaction with β -amyloid and leads to pathogenesis of AD [35]. From the recent studies benzothiazole hybrids considered as good AChE inhibitors also fluoro derivatives of benzothiazole proved as potent inhibitor AChE and butyrylcholinesterase (BChE) [36], few more methyl, ethyl, methoxy, chloro substituted benzothiazole has been reported from the recent research which has been evaluated as moderate AChE inhibitor [37].

1.5.2 Hydroxypyridinone

The hydroxypyridinone moiety, or more specifically the 3-hydroxy-4-pyridinone, is also a heterocyclic i.e. pyridine ring with hydroxy and keto substitution (**Scheme 3**). From the very previous time this moiety has been proved as a class of an antimycotics i.e. antifungal in nature [38] and in the recent studies pyridone derivatives were found to possesses good anti-HIV activities [39]. Pyridone derivatives have been also reported as anti-tumor, anti-oxidant and hard metal ion chelator [40] one of the well-known hydroxypyridinone, i.e. deferiprone (DFP), has been proved as very good tridententate

iron chelator [40], and from the recent studies it has been proved that disturbed homeostasis of metals (Fe, Cu, Zn) in the brain contribute to AD. Further derivatives of DFP also have been investigated as good inhibitor of beta amyloid aggregation and also used as prodrug against AD [41]. Also from the recent researches it has been concluded that, if mono-hydroxypyridinone-base ligands are further extrafunctionized, they could act as a multitarget molecule to tackle the various known disease targets, including acetylcholinesterase, oxidative stress and β -amyloid ($A\beta$) aggregation [42]. So because of anti-oxidant and metal chelating properties derivatives of hydroxypyridinones, they were also synthesized in the present work, conjugated with known tacrine, and then investigated against AD through various assays.

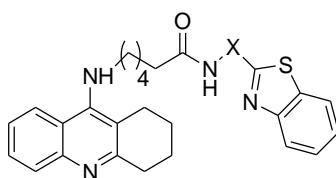


Scheme 3. Moieties used to synthesize the studied hybrids (tacrine, benzothiazole, hydroxypyridinone)

2. Literature review

2.1 Tacrine-benzothiazole series

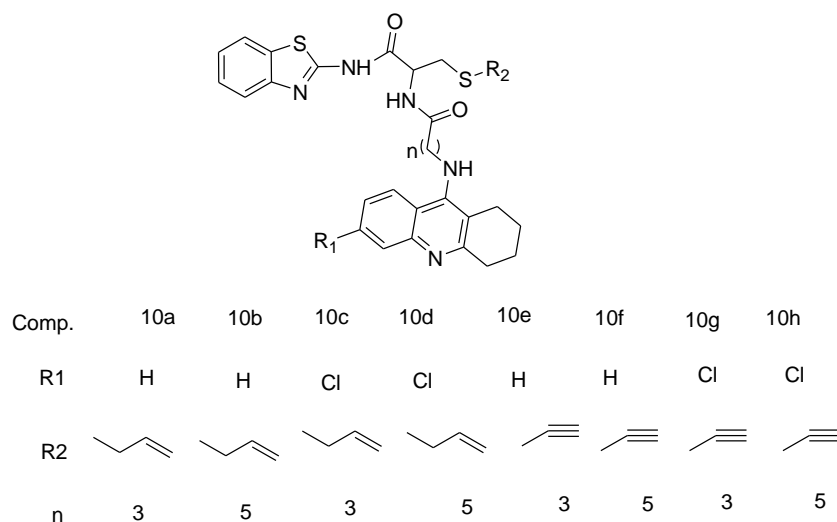
From the recent literature review, some TAC-BTA hybrids have been developed [43], and evaluated for AChE inhibition and A β aggregation inhibition. It has been concluded that they have potent activities in all assays. The common structure of derivatives (7a-7e) is presented in **Scheme 4**, the best AChE inhibitor was reported compound 7a (IC₅₀ = 0.34 μ M) with phenyl linker between two moieties, but the remaining compounds were quite good inhibitor with the IC₅₀ in the range (0.57 \pm 0.1 μ M to 1.84 \pm 0.2 μ M), in the A β aggregation inhibition, compound 7b showed max inhibition (61.3%, with 80 μ M) as compare to the reference compound tacrine (11%, with 80 μ M), while remaining compounds are also much better than tacrine i.e. (22-35%), Also, two compounds 7a and 7d proved to have good antioxidant activity.



Comp code	X
7a	Ph
7b	PhCH ₂
7c	CH ₂ PH ₂
7d	(CH ₂) ₃
7e	(CH ₂) ₅

Scheme 4. (7a-7e) Representation of tacrine- benzothiazole derivative. [43]

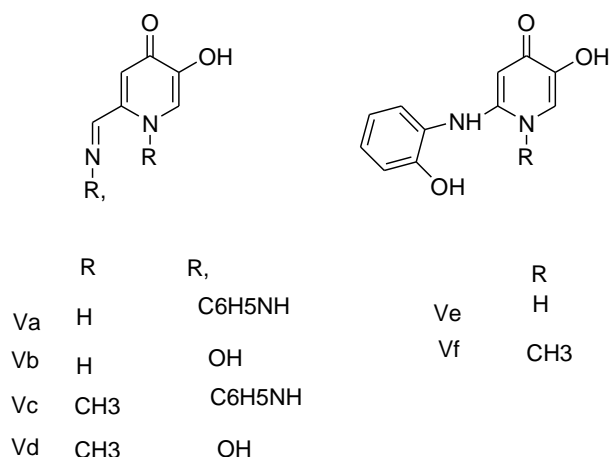
Two series of tacrine-S-allylcysteine-benzothiazole (TAC-SAC-BTA) and tacrine-S-propargylcysteine-benzothiazole (TAC-SPRC-BTA) has also been reported in the literature [44], and it was found that all of these hybrids (see **Scheme 5**) 10a-10h were comparable with the parent tacrine in the AChE inhibition i.e. in the range of (IC₅₀ = 0.25-0.37 μ M), also few compounds were concluded as good inhibitors of A β ₁₋₄₂ self-aggregation i.e. 10a (59%), 10b (78%), 10f (56%), although they were not good antioxidant compounds i.e. comparable to tacrine (IC₅₀ >1000 μ M).



Scheme 5. Representation of tacrine–S-allylcysteine–benzothiazole (TAC–SAC–BTA) and tacrine–S-propargylcysteine–benzothiazole (TAC–SPRC–BTA) hybrids. [44]

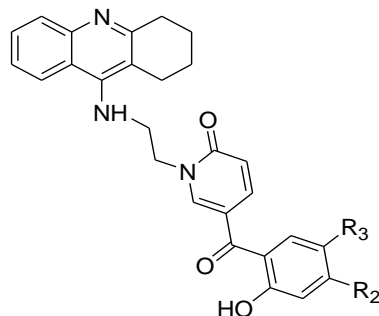
2.2 Hydroxypyridone-based anti-neurodegenerative agents

From the recent literature view, hydroxypyridinone derivatives have been reported as strong chelator of hard metal ions as well as to take part in the redistribution of misplaced metal ions in certain organs, for example the brain of patients with some neurodegenerative diseases [45]. As we knew already from the recent research that hydroxypyridinones (HP) being a benzenoid N-heterocyclic with ortho-positioned hydroxyl and ketone groups, stabilized itself in three types i.e. 1,2-HP, 3,2-HP and 3,4-HP, as shown in **Scheme 6**. All these types of HPs have high selectivity for trivalent metal ions over divalent biometals [46]. A series of hydroxypyridinone derivatives, with quite good antioxidant potential, has been reported [47] and the HP derivatives Va–V_f are presented in **Scheme 6**. Compounds Va ($IC_{50} = 0.013$ mg/ml), Vb ($IC_{50} = 0.021$ mg/ml) and Ve ($IC_{50} = 0.013$ mg/ml) were reported as good antioxidant compounds without any substitution at N¹ atom of the pyridinone ring so that it can donate hydrogen to stabilize the free radical, as compare to others with some kind of substitutions on N¹ atom of the pyridinone, among all Va ($IC_{50} = 0.013$ mg/ml) concluded as more potent in antioxidant activity. All these compounds also reported to show good Fe chelating ability.



Scheme 6. Derivatives of hydroxypyridone. [47]

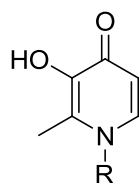
Another series related with hydroxypyridinones, designed in accordance with multi-target approach against AD, are the tacrine-(hydroxy benzoyl-pyridone) hybrids recently reported in literature [48]. Analysis of the results of bioassays for these hybrids it was concluded that these tacrine-(hydroxy benzoyl-pyridone) (**Scheme 7**) have AChE inhibition potential in the range of ($IC_{50} = 0.57-0.78 \mu M$), which were quite comparable to the reference or parent moiety tacrine; also they were quite good anti-oxidants, as they exhibit antioxidant values in the range ($EC_{50} = 204-249 \mu M$).



Comp	R2	R3	n
15	OMe	H	1
16	H	OMe	1
17	OH	H	3

Scheme 7. Representation of tacrine-(hydroxybenzoyl-pyridone) hybrids. [48]

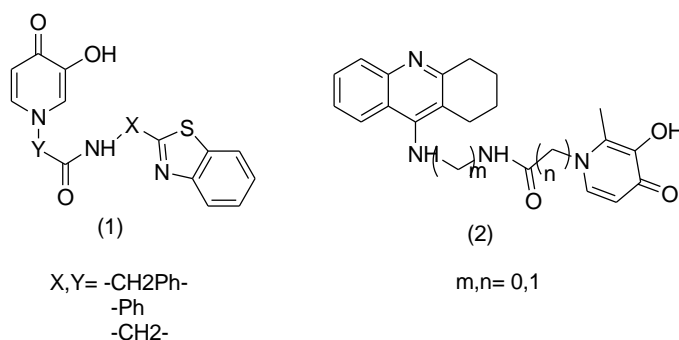
Another series of 3-hydroxy-4-pyridinones derivatives, as shown in **Scheme 8**, have also been reported for their potential activities against AD [49]. Anti-oxidant capacity of these 3-hydroxy-4-pyridinones derivatives were concluded as almost equivalent to the reference drug Trolox i.e. analogue of α -tocopherol, also in the A β aggregate resolubilization assay these compounds 2b and 4b reported to have inhibitory potential against Zinc(II) and copper(II) induced A β aggregation.



Comp. code	R
2b	Methyl
3b	Hexyl
4b	Phenyl
5b	4 (isobutyl)phenyl

Scheme 8. Representation of 3-hydroxy-4-pyridinones derivatives. [49]

Very recent literature has also been reported on HP derivatives as anti-neurodegenerative drugs [42], in which series of mono-HP hybrids were synthesized on the basis of multifunctionalization of mono HP (see **Scheme 9**). They include the functionalization of mono HP with benzothiazole (1), which showed good interactions with the cross- β sheet structure of (A β) fibrils and inhibit their aggregation; also the functionalization of mono HP with tacrine (2) were reported to have much potent AChE inhibitory activity, and being HP compounds they have already good metal chelating and radical scavenging ability.



Scheme 9. Representation of mono-HP functionalized hybrids. [42]

This literature review is very specific, focusing on the moieties that have been used to synthesize the compounds of the present thesis work. It would be very helpful to get a multifunctional drug against AD, because all used moieties have proved to be active in different biological assays against AD, but we also know that, in spite of numerous research efforts, AD is still an incurable disease. Based on literature results relatively to synthesis and biological investigation of such type of tacrine derivatives against AD, namely antioxidant activity, AChE inhibition and (A β) peptides aggregation inhibition, it is possible to conclude that tacrine hybrids could be a good approach against AD.

3. Aim of present work (Thesis)

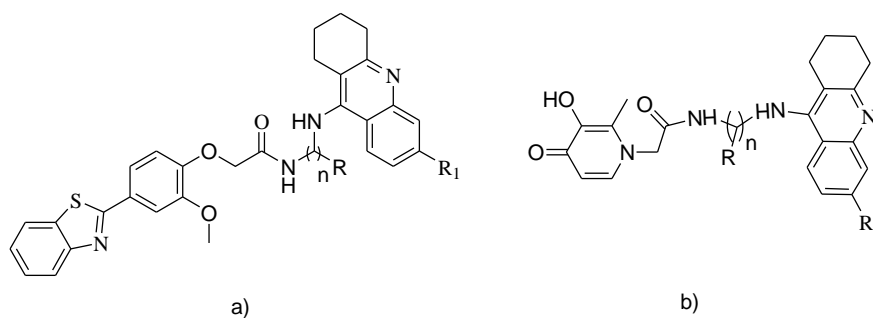
Two series of compounds were synthesized and investigated in the present work, under a similar approach, i.e. hybridization of tacrine with methoxyphenyl-benzothiazole or hydroxypyridinone moieties with different carbon chain length linkers.

The aim of the present thesis work lies on a multi-target approach towards the development of drugs against the multifactorial AD, because it is difficult to tackle AD with a single target approach, as it has been proved that multiple factors are involved in the pathogenesis of this disease. In the past, many scientists failed to overcome this disease with single inhibitory approach and so the present work was planned and applied and investigated in accordance with a multi-target approach. From literature results, it is known that AChE is responsible for the hydrolysis of ACh at its catalytic anionic site (CAS) and that it promotes the aggregation of A β ₁₋₄₂ at its peripheral anionic binding site (PAS). So, dual binding site inhibitors of AChE could be beneficial and promising factors in relieving symptoms of AD by reducing both ACh hydrolysis and A β ₁₋₄₂ aggregation [43].

So, based on this fact, both herein studied series of tacrine derivatives, as shown in **Scheme 10**, with adequate linker size/type, i.e. carbon spacer and substituent OH, could improve the inhibitory potential by a bimodal interaction with both active sites of AChE enzyme, i.e. CAS and PAS. In fact, the methoxyphenylbenzothiazole or hydroxypyridinone moieties are able to interact with the PAS, by forming aromatic stacking with amino acids of this active site, thus allowing strong interactions with the enzyme, and the tacrine moiety is always found well inserted in the CAS by π - π stacking with the aromatic ring of amino acids of this active site [50, 51]. Also it has been reported that peripheral anionic site (PAS) of the AChE is capable to promote aggregation and deposition of the A β peptides; from the molecular modeling, it was suggested that the methoxyphenylbenzothiazole and methylhydroxypyridone moieties of these hybrid compounds could have good interaction with the amino acids of PAS, via aromatic π -stacking; so inhibition of functioning of PAS would be good for (A β) peptides aggregation inhibition, also on the basis of fact that AChE catalytic gorge possesses strong lipophilic character in that respect interacts much better with the more hydrophobic synthetic inhibitors [51]. Herein, the used methoxyphenylbenzothiazole moiety, with increased hydrophobic character, as compared with the benzothiazole, because of methoxyphenyl substitution, would be expected to present a better interaction with AChE and concomitant increase of AChE inhibition and (A β) peptide aggregation instead of simple benzothiazole moiety.

Hydroxypyridinones are very efficient in chelating therapy, because of their high affinity for a range of metal ions as and form stable complexes with trivalent cations such as iron(III) and aluminum(III); the chelating capacity depend on the arrangement of the (O,O) donor groups around the central pyridine ring. As in the present case it is a 3,4-HP moiety, that arrangement provides to the hydroxyl group the highest basicity (pK_a ca. 9-9.5), and so highest electronic density at the coordinating atoms, leading to neutral compounds at physiological pH, which results in higher affinity for heavy metal ions (e.g. Fe³⁺) rather than the biologically important bivalent metal ions (e.g. Fe²⁺, Zn²⁺, Cu²⁺). These hybrids of both series have also the ability to act as antioxidants by their hydrogen donating ability through the OH functional group. So, the derivatives of both series should have ability

to tackle various pathological aspects of AD, being good antioxidants, quite good inhibitors of AChE, and few of them are also very potent A β ₁₋₄₂ aggregation inhibitors as well as good metal chelator.



Scheme 10. Representation of general structure of both present studied series; a) Tacrine-methoxyphenylbenzothiazole ($n = 2,3$; $R = H, OH$ and $R_1 = H, Cl$); b) Tacrine-hydroxypyridinones ($n = 2,3,4$; $R = H, OH$ and $R_1 = H, Cl$)

4. Discussion of results

4.1 Molecular modeling

Docking studies of the TAC-BTA and TAC-HP hybrids into the active site of the enzyme involved in cholinergic loss i.e. AChE, were performed in order to know what are the type of interactions eventually established between this enzyme and the proposed hybrid molecule so that we can predict the binding modes. AChE enzyme contains a deep pocket, at the bottom of which is located the catalytic site, known as the 'catalytic triad' of AChE formed by three amino acids, Ser200, His440 and Glu327 (sequence numbering of *Torpedo californica* AChE, TcAChE) [52]. Apart from this, it possesses two more active sites CAS and PAS. Three important amino acids, Phe330, Trp84 and Glu199 forms CAS which is situated at the lower part of the gorge, while PAS located at the entrance of the gorge is formed by Trp279, Asp72 and Tyr70 [52]. It is known from previous studies that in this deep pocket of the AChE enzyme, acetylcholine (substrate) can slip inside with water molecule and get hydrolyzed into acetic acid and choline, which after hydrolysis no longer remains a neurotransmitter and contributes towards AD progression. The compounds which have the capability to interact at both CAS and PAS site of the enzyme can fill up this deep pocket and have proved to be good AChE inhibitors.

Therefore, the strategy followed herein for the design of new potential AChE inhibitors was the coupling of two main moieties- TAC and BTA or TAC and HP - unit through an alkyl spacer in such a way that one moiety can interact with CAS while at the same time other moiety can interact with the PAS and produces maximum AChE inhibition. Therefore, the length of the alkyl spacer between the selected two moieties of the designed inhibitors was decided by the docking study using program GOLD, v. 5.1. [53]. The crystal structure of TcAChE complexed with an inhibitor was taken from RCSB Protein Data Bank (PDB, entry 1ODC) [54]. This structure was chosen because of the similarity between its inhibitor and the synthesized ligands. The original ligand (*N*-quinolin-4-yl-*N*-(1,2,3,4-tetrahydroacridin-9-yl)octane-1,8-diamine) [43] is formed by tacrine connected through a long carbon chain to an aminoquinoline moiety, which is structurally very similar to the phenylbenzothiazole moiety containing phenyl ring attached to benzothiazole. The docking calculations were performed using the ASP scoring function, since this function has previously proven to give the best docking predictions for AChE inhibitors [6, 7, 51].

The docking studies revealed favorable interactions for the new inhibitors with many similarities in their binding conformations. **(Figure 2) (RSC-3)** and **(Figure 3) (TACHP-12)** show that the ligands are well inserted into the cavity of the active site, blocking the entrance to the substrate (choline) and water molecules. The TAC moiety is always found well inserted in the bottom of the gorge of the enzyme, binding to the CAS by π - π stacking with the aromatic ring of Trp84 and Phe330, overlapping almost perfectly with the TAC moiety of the original ligand. Generally, the alkyl spacer along with the methoxyphenylbenzothiazole rings, in case of TAC-BTA series, and the hydroxypyridone rings, in TAC-HP compounds, seems to be well accommodated along the hydrophobic cavity, and were always placed at the entrance of the gorge, being lipophilic in nature due

the presence of 'methoxy' and 'methyl' kind of lipophilic substitution, able to bind with PAS forming aromatic stacking interaction with Tyr70 and Trp279, allowing the maintenance of strong interactions with the enzyme.

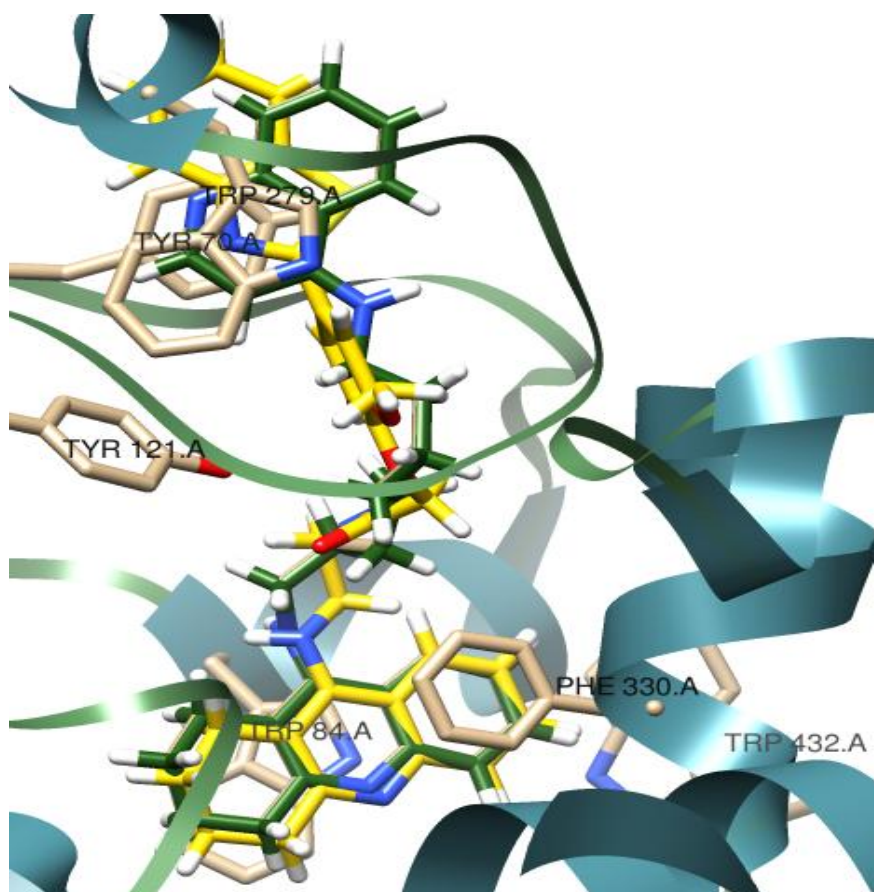


Figure 2. Docking results for the TAC-BTA hybrids with AChE: superimposition of **RSC-3** (yellow) with original ligand (green)

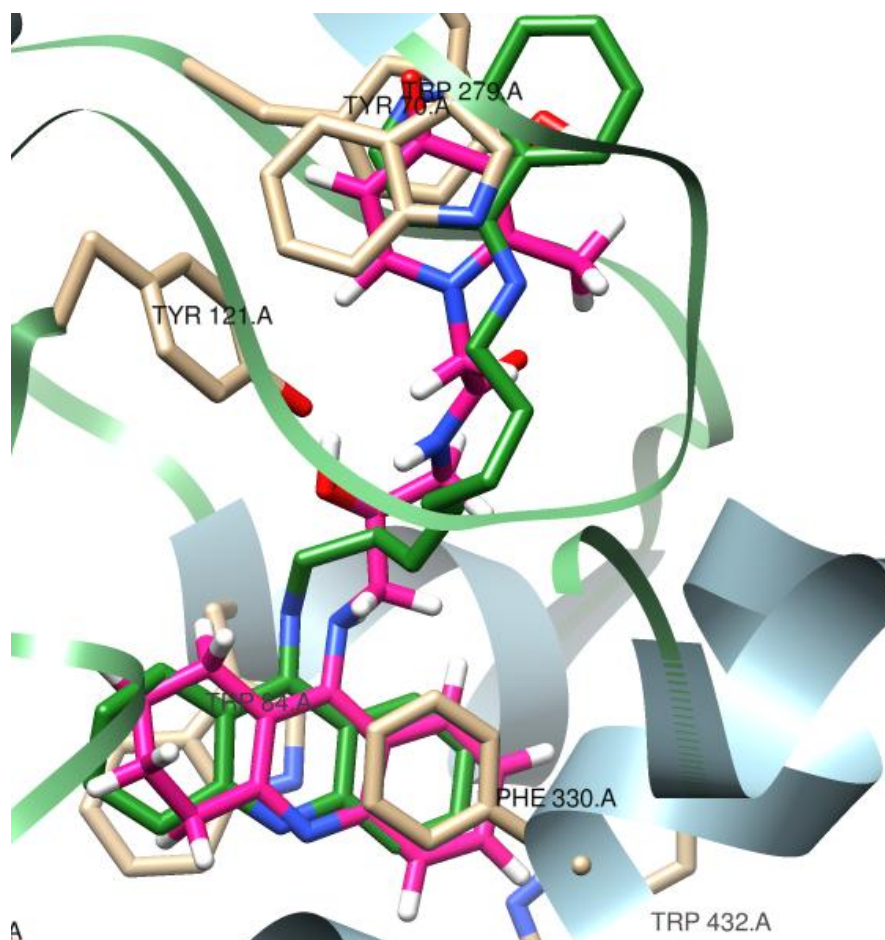
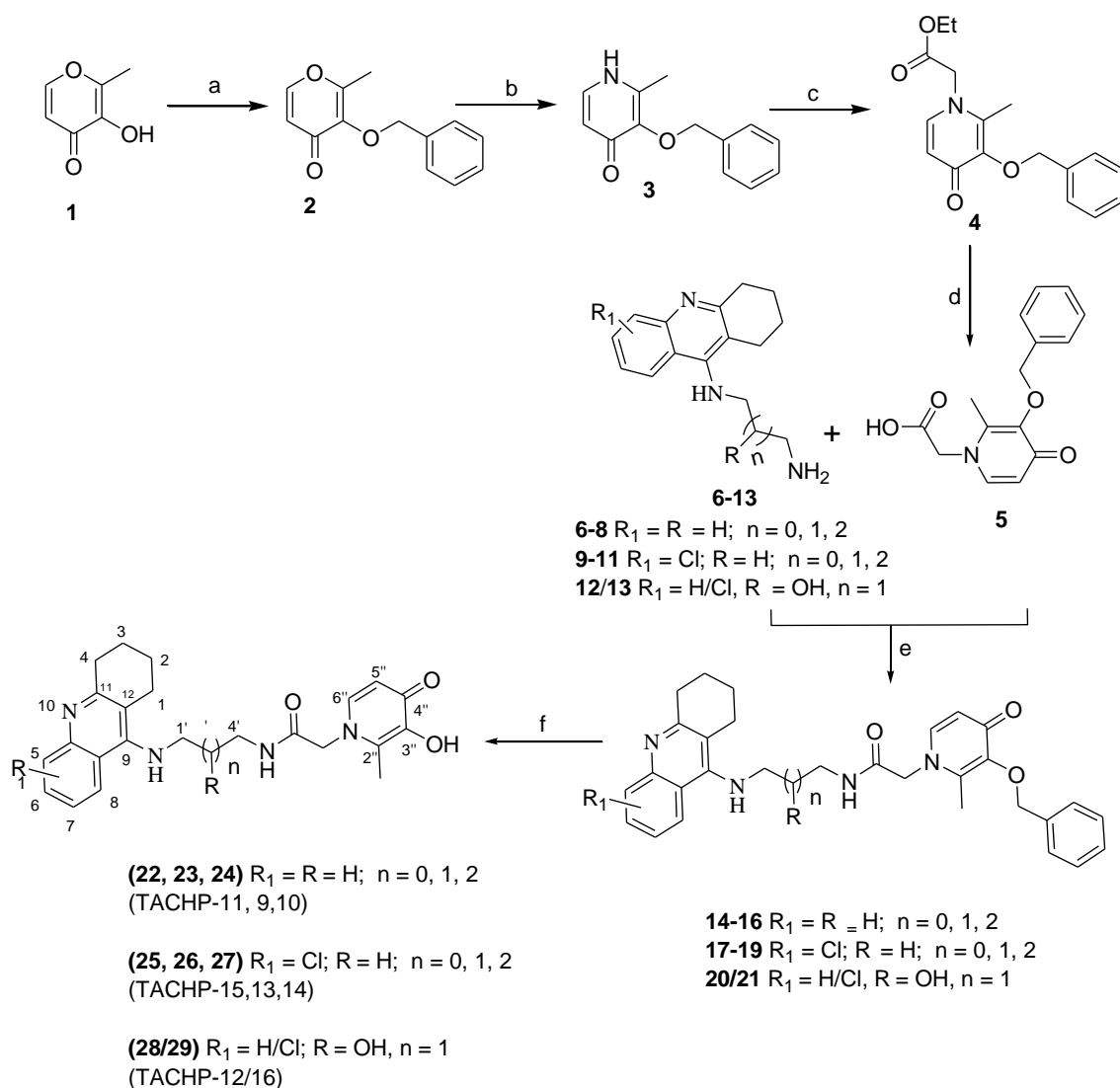


Figure 3. Docking results for the TACHP hybrids with AChE: superimposition of **TACHP-12** (pink) with original ligand (green)

4.2 Chemistry

The tacrine-benzothiazole hybrids (**RSC-1** to **RSC-6**) were not synthesized under the framework of this thesis. The tacrine-hydroxypyridone (**TACHP-9** to **TACHP-16**) hybrids were synthesized according to shown in **Scheme 11**. It involved the previous synthesis of an *N*-carboxylic derivative of hydroxypyridinone (**5**) followed by its attachment to alkylamine-tacrine derivatives. The preparation of compound **5** involved 4 steps. Firstly, the commercial available pyrone, 3-hydroxy-2-methyl-pyran-4-one, was *O*-benzylated (**2**) by the refluxing with benzylchloride in a mixture of NaOH aqueous solution and MeOH. Afterwards, the protected pyrone (**2**) was transformed in the corresponding hydroxypyridinone (**3**) by its reflux in a mixture of NH₃ and ethanol. Then, the heterocyclic amine group of (**3**) was attached to acetyl ester through nucleophilic substitution with ClCH₂COOEt and K₂CO₃ in DMF, to provide compound (**4**). Further hydrolysis of compound (**4**), in the presence of NaOH in MeOH and H₂O, afforded compound (**5**). Compound (**5**) was coupled with the previously synthesized alkylamine-tacrine intermediates (**6-13**), in the presence of base (NMM) and

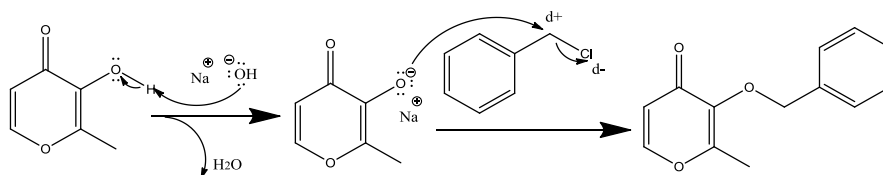
coupling agent T3P in dry DCM, to provide (**14-21**). The benzyl groups of these pre-final intermediates were further removed by hydrogenolysis with, H₂, Pd/C in MeOH to get the final compounds (**22-29**) i.e. (**TACHP-9 to 16**).



Scheme 11. Reagents and conditions: a) MeOH, NaOH (1.1eq), benzyl chloride, reflux; b) Ethanol, Ammonia (28%) reflux; c) anhydrous DMF, K_2CO_3 , $ClCH_2COOEt$; d) MeOH, NaOH, H_2O ; e) anhydrous DCM, NMM, T3P, RT, 7-8 h; f) MeOH, H_2 (2 bar), Pd/C.

4.2.1 Mechanism

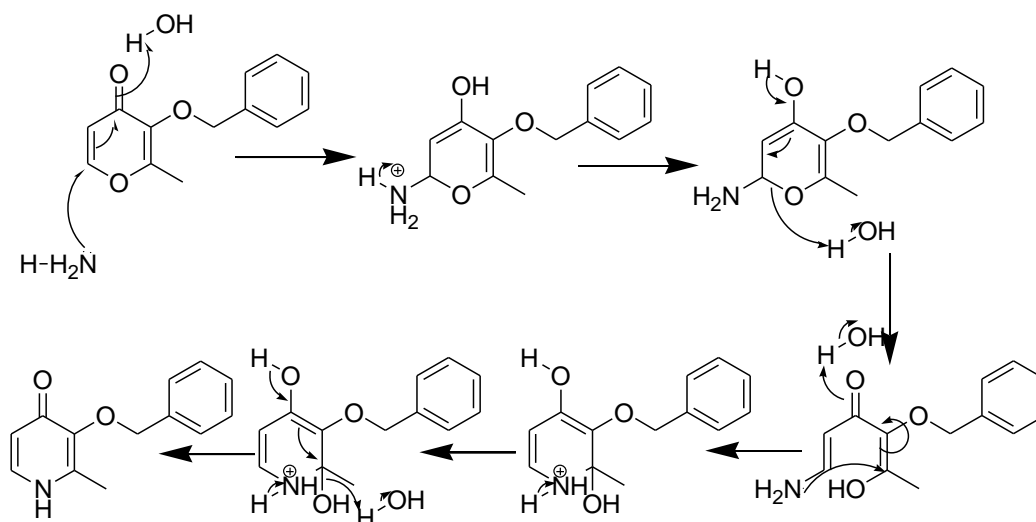
First step of the synthesis involves the protection of hydroxyl group with the benzyl group, by nucleophilic substitution, which mechanism is presented in **Scheme 12**.



Scheme 12. Mechanism of OH protection

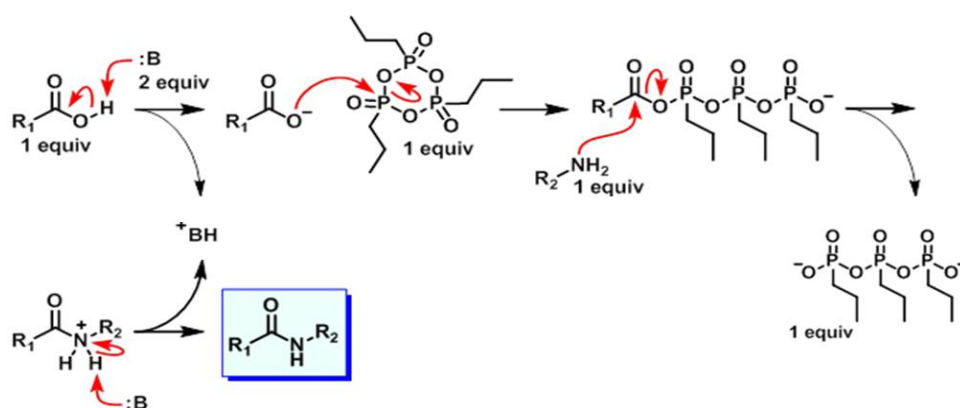
In the work up excess of inorganic salt was filtered, and the filtrate so obtained was concentrated under reduced pressure and dissolved in CH_2Cl_2 and washed with 5% NaOH to remove the excess of starting material i.e. maltol.

The second step of the synthesis follows the mechanism of Michael-type addition reaction which involves the opening and closing of the ring, as shown in **Scheme 13**.



Scheme 13. Mechanism of Michael type addition reaction

The carboxylic-amine coupling reactions (amide bond formation) to obtain the pre-final compounds (**14-21**), (**Scheme.14**), were performed with T3P coupling reagent. The mechanism of this coupling proceeds with the action of base in the deprotonation of carboxylic acid, and the so formed carboxylate anion attacks on T3P and forms an active T3P-carboxylic ester intermediate. The carbonyl group of this active intermediate is attacked by the amine group, as shown in **Scheme 14**. Excess of T3P and polyphosphonate derivative of the leaving group get removed in water along the reaction work up.



Scheme 14. Acid-amine coupling mechanism

4.3 Biological studies

4.3.1 TAC-BTA series

Biological evaluation of the TAC-BTA derivatives (**RSC-1** to **RSC-6**) towards inhibition of AChE and A β_{1-42} self-aggregation has been performed. Pharmacokinetics properties were also determined using QIKPROP v. 2.5 [55] provided by MAESTRO [56], and so now we will discuss the results of the above referred assays.

4.3.1.1 Acetylcholinesterase inhibition assay

In order to determine the potential of these hybrid compounds towards AChE inhibition, all hybrids **RSC-1** to **RSC-6** were investigated by a modified method of Ellman *et al* [43]. Compound **RSC-1** shows an IC₅₀ value of 0.15 μ M, **RSC-2** 0.13 μ M, **RSC-3** 0.12 μ M, **RSC-4** 0.05 μ M, **RSC-5** 0.14 μ M and **RSC-6** 0.27 μ M. From the obtained results it is possible to conclude that all the compounds are better in terms of inhibition of *electric eel* AChE than the reference compound tacrine (IC₅₀ = 0.30 μ M). Moreover, the TAC-BTA hybrids with chloro (Cl) substitution on the TAC moiety proved to be better inhibitors than the corresponding analogues without Cl group (and the same chain length of carbon linker between TAC and BTA). This can be observed for the pairs of compounds **RSC-1/RSC-2**, with three carbon atoms in the linker, **RSC-3 /RSC-4**, with two carbon atoms in the linker, or **RSC-5/RSC-6**, where a hydroxyl group has been further introduced in a three carbon linker chain. So the TAC-BTA derivative with two carbon chain linker and chloro substitution on the phenyl ring of TAC, i.e. **RSC-4** (IC₅₀ 0.05 μ M), was found to be the best inhibitor of *electric eel* AChE for this series of compounds. The set of results obtained for the assays performed with compounds TAC-BTA are summarized in **Table 1**.

4.3.1.2 Inhibition of amyloid beta self-aggregation

All TAC-BTA hybrids (**RSC-1** to **6**) were tested for their potential to inhibit the amyloid β_{1-42} self-aggregation by Thioflavin-T fluorescence method and the results compared to those of the reference compound TAC (see **Table 1**). Since the compounds of this series presented some solubility problems in methanol, the assays were performed with ligand concentration 40 μ M, i.e. half of the concentration usually used in these assays. Therefore, reference compound TAC was used in both 80 μ M and 40 μ M, in order to compare the obtained values. Compounds (**RSC-1** to **6**) show percent of inhibition values for A β self-aggregation in the range 27-44.6%, while tacrine presented a value of 11% that was independent of the value of the ligand concentration. From the results it is possible to verify that all these TAC-BTA hybrids are moderate inhibitors of amyloid β_{1-42} self-aggregation although better than the reference compound TAC. Among these hybrids, **RSC-3** (44.6%), with a two carbon linker between TAC and BTA moieties and without Cl substitution in TAC, seems to allow the best interaction of the BTA moiety with β -sheet secondary structure of amyloid-beta aggregates. Cl substitution on the phenyl ring of TAC, with the same chain length of carbon linker, reduces the inhibition percentage of **RSC-3** to 27.0% **RSC-4**. Chloro substitution also decreases the inhibition capacity for the compounds with three carbon chain linker, i.e. **RSC-2** versus **RSC-1**, while further hydroxyl group introduction in the three carbon linker was found to attenuate

differences in the inhibitory capacity for the pair **RSC-5/RSC-6** (ca 31%). So, the introduction of chloro substituent in TAC and/or hydroxyl group in carbon linker maybe is not well suited for the interaction with β -sheet secondary structure of amyloid-beta aggregates. But still all these hybrids are better than tacrine, so we can say that these hybrids, composed of biaryl heterocyclic groups, are able to recognize and interact with the abnormal β -sheet conformation of the A β peptide, and to induce the inhibition of the fibril genesis.

4.3.1.3 Pharmacokinetic characterization

In the pharmacokinetic study, parameters such as the lipo-hydrophilic character ($\text{clog } P$), the ability to cross the blood-brain barrier ($\log \text{BB}$) and the ability to be absorbed from the intestinal tract to the blood (Caco-2 cell permeability), were calculated along with verification of Lipinski's rule of five [57]. As it can be seen in **Table 1**, all the compounds present $\text{clog } P$ (octanol/water) coefficients superior to five, while **RSC-2** is even greater than 6.5, which means that this set of compounds have a lipophilic character higher than recommended by Lipinski's rule. All compounds also have molecular weights higher than 500, even higher than 600 for **RSC-5**, which accounts for two violations of this rule. Concerning Caco-2 permeability, some compounds (**RSC-1,2,3,4**) exhibited very good results, ranging from ca 700-1086 nm/sec (higher than 500 nm/sec is considered good [55], indicating that the absorption through the intestinal tract to the blood is possible. Nevertheless, compounds **RSC-5** and **6** have values lower than 500 nm/sec which precludes lower absorption through intestinal tract to the blood.

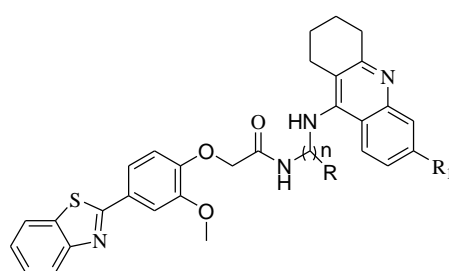
Finally, the high lipophilic character and the low blood-brain barrier permeability ($\log \text{BB}$) provides a conclusion that all these compounds are not eligible drug candidates for oral administration, and require further improvement to ameliorate compound absorption and entering into the cells.

Table 1. Summary of activities of TAC-BTA derivatives (**RSC-1** to **RSC-6**) towards radical scavenging (DPPH), inhibition of AChE and A β_{1-42} self-aggregation and Predicted pharmacokinetic values for TAC-BTA hybrids^a

Comp. Code	R ₁	DPPH Scavenging (EC ₅₀ , μM) ^b	AChE (IC ₅₀ , μM) ^c	Inhibition of A β -self-aggregation (%) ^{d,e}	MW	$\text{clog } P$ ^f	$\log \text{BB}$ ^g	Caco-2 Permeability (nm/sec)	Violations of Lipinski's rule of 5	CNS activity
RSC-1	H	> 1500	0.15	33.7	552.69	6.237	-0.975	1057	2	-
RSC-2	Cl	> 1500	0.13	32.5	587.13	6.726	-0.739	1022	2	-
RSC-3	H	Nd*	0.12	44.6	538.66	6.200	-0.927	1086	2	-
RSC-4	Cl	Nd*	0.06	27.0	573.10	5.445	-0.914	722	2	-

RSC-5	Cl	Nd*	0.14	31.3	603.13	5.692	-1.268	496	2	-
RSC-6	H	>1500	0.27	31.1	568.60	5.222	-1.592	388	2	-
TAC	-	>1000	0.30	11	198.1	-	-	-	-	-

^aPredicted values using program QikProp v. 2.5. K [55]; ^bCapacity to scavenge the stable free radical 2,2-diphenyl-1-picrylhydrazyl (DPPH) was monitored according to the Blois method [58] (EC₅₀, μM) (means of two experiments)(see **section 4.4**); ^cAChE from *electric eel*, IC₅₀, inhibitor concentration (means of two experiments) for 50% inactivation of AChE; ^dInhibition of self-mediated Aβ₄₂ aggregation (means of two experiments). The Thioflavin-T fluorescence method was used, and the measurements were carried out in the presence of an inhibitor; ^eAssays performed with C_L = 40 μM; *Not determined due to very poor solubility in methanol; ^fCalculated octanol/water partition coefficient; ^gBrain/blood partition coefficient.



	RSC-1	RSC-2	RSC-3	RSC-4	RSC-5	RSC-6
R ₁	H	Cl	H	Cl	Cl	H
n	3	3	2	2	3	3
R	H	H	H	H	OH	OH

Scheme 15. Representation of derivatives of TAC-BTA

4.3.2 TACHP series

Evaluation of the TACHP derivatives (**TACHP-9** to**16**) towards radical scavenging (DPPH), inhibition of AChE and Aβ₁₋₄₂ self-aggregation has been performed. Pharmacokinetics properties were also determined using QIKPROP v. 2.5 [55] provided by MAESTRO [56].

4.3.2.1 Acetylcholinesterase inhibition

In order to determine the potential of these hybrids towards AChE inhibition, all TACHP compounds were assayed by modified method of Ellman *et al* [43, 52]. It was found that the compound with three carbon chain linker between TAC amine and HP, i.e. **TACHP-9**, has a better IC₅₀ value (0.90 μM) than the compound with four carbon linker (**TACHP-10**, IC₅₀ = 1.71 μM) or with two carbon linker (**TACHP-11**, IC₅₀ = 1.07 μM). Moreover, **TACHP-12** (IC₅₀ = 0.96 μM), with three carbon linker containing hydroxyl group, shows better inhibition, similar to**TACHP-9**. So, the hydroxyl group is

not responsible for an enhancement of the inhibitory potential of the compound with three carbon linker. Compound **TACHP-13** ($IC_{50} = 0.86 \mu\text{M}$), with three carbon linker and chloro-substitution at phenyl ring of TAC, presents a quite good AChE inhibition capacity, while **TACHP-14** ($IC_{50} = 1.01 \mu\text{M}$), with four carbon chain linker and chloro substitution at TAC is a better inhibitor than its analogue **TACHP-10**, with the same carbon linker but without chloro substitution. Compound **TACHP-15** ($IC_{50} = 0.97 \mu\text{M}$), with ethyl linkage and chloro substitution, is similar to **TACHP-11**. Finally, compound **TACHP-16** ($IC_{50} = 0.64 \mu\text{M}$), with three carbon chain linker and both chloro and hydroxy substitution, shows the best inhibitory activity among all analogues of this series.

Therefore, it was demonstrated that the chlorosubstitution at the phenyl ring of tacrine increases AChE inhibition, besides the existence of a three carbon linker being necessary to better accommodate the inhibitor molecule in the reactive sites of AChE. Even though hydroxy substitution in the linker was found to decrease the inhibition potential, in the case of **TACHP-16** both hydroxyl and chloro groups seem to contribute to the increase of the inhibition capacity.

4.3.2.2 Inhibition of amyloid beta aggregation

All TACHP hybrids (**TACHP-9** to **TACHP-16**) were tested for their potential to inhibit the amyloid β_{1-42} self-aggregation by Thioflavin-T fluorescence method in comparison to the reference compound tacrine. So, as shown in **Table 2**, all these derivatives proved to have a very high inhibitory capacity (ca 85-95%) of amyloid β_{1-42} self-aggregation, when compared with the reference compound tacrine. Two of the compounds of this series were also checked for copper (Cu^{2+}) self-mediated inhibition of aggregation: **TACHP-9** (94.8%) and **TACHP-12** (54.0), in (Cu^{2+}) self-mediated inhibition of aggregation assay, **TACHP-9** without substituted linker was proved good inhibitor because only pyridyl OH involves in metal chelation, not OH of alkyl linker, also non substituted alkyl linker compounds reported to have better amyloid β_{1-42} self-aggregation inhibition as compare to substituted alkyl linker compounds [59].

In order to try to gain support for the rationalization of the obtained results in terms of the effect of the hybrids on the inhibition of $\text{A}\beta_{1-42}$ aggregation instead of their competition with ThT for fibril binding, independent transmission electron microscopy (TEM) assays were performed (see **Figure 4**) with one model compound, **TACHP-12**. The visualization of the fibrils by TEM shows the presence of heavily intertwined networks for $\text{A}\beta_{1-42}$ alone and in the presence of copper, while in the presence of ligand **TACHP-12** the aggregates become sparser. Although these results point to the role of these hybrid compounds as inhibitors of $\text{A}\beta_{1-42}$ aggregation, they are not clear about the role of Cu(II) .

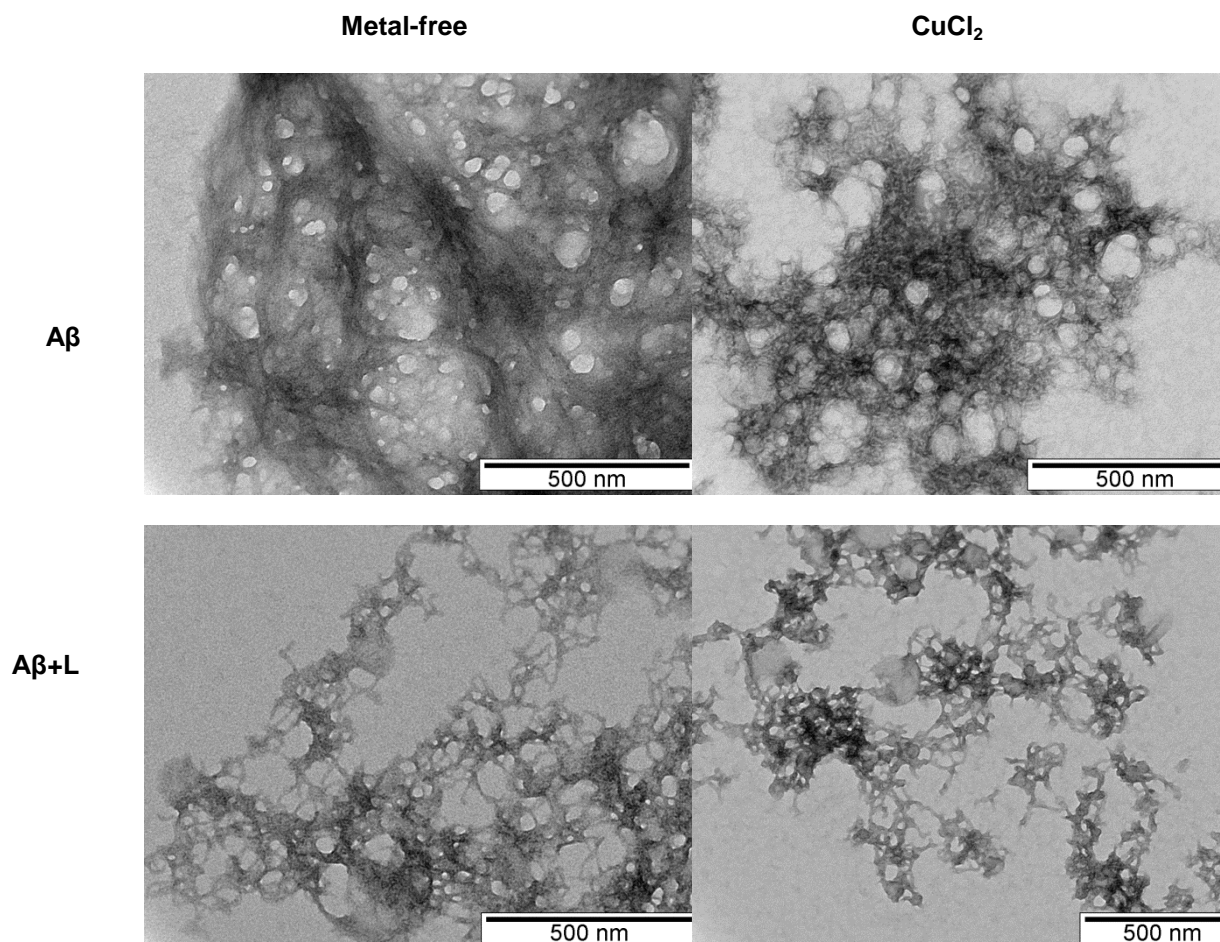


Figure 4. TEM images of A β -aggregation inhibition experiments performed with samples incubated (37 °C) for 24 h. Experimental conditions: [A β ₄₂] = [CuCl₂] = 25 μ M; [TACHP-12] = 50 μ M; pH 6.6.

4.3.2.3 Pharmacokinetic characterization

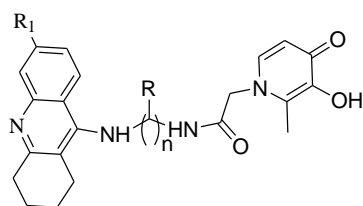
In the pharmacokinetic study, the determined parameters were calculated along with verification of Lipinski's rule of five and the results are contained in **Table 2**. All the compounds presented *clog P* (octanol/water) coefficients inferior to five, approximately in the range 1-3, which is considered to be good in order to penetrate the cell membrane and maintain water solubility. This range of *clog P* values leads this set of compounds to have a balance character between lipophilic and hydrophilic character recommended by Lipinski's rule. All compounds also have molecular weights lower than 500, which is also in accordance with Lipinski's rule [57]. Nevertheless, concerning Caco-2 permeability, all compounds (**TACHP-9** to **16**) exhibit poor results, ranging from ca. 66 to 260 nm/sec (higher than 500 nm/sec is considered good [55]), indicating that the absorption through the intestinal tract to the blood would be very poor. As a conclusion, the balanced lipophilic/hydrophilic character and the low blood-brain barrier permeability (log BB) point towards the possible eligibility of all these

compounds as drug candidates for oral administration, although requiring further improvement to ameliorate compound absorption through blood in intestinal tract and entering into the cells.

Table 2. Activities of the TACHP derivatives (**TACHP-9** to **TACHP-16**) towards radical scavenging (DPPH), inhibition of AChE and A β ₁₋₄₂ aggregation and predicted pharmacokinetic values for TACHP hybrids^a

Comp. Code	R ₁	DPPH scavenging (EC ₅₀ , μM) ^b	AChE (IC ₅₀ , μM) ^c	Inhibition of A β self-aggregation(%) ^{d,e}	MW	clog P ^f	log BB ^g	Caco-2 Permeability (nm/sec)	Violations of Lipinski's rule of 5	CNS activity
TACHP-9	H	925±8	0.90	85.3 Cu/94.8	420.51	2.745	-1.739	154	0	--
TACHP-10	H	450±8	1.71	89.1	434.53	3.128	-1.941	139	0	--
TACHP-11	H	> 1200	1.07	88.1	406.48	2.531	-1.494	230	0	--
TACHP-12	H	399±5	0.96	86.0 Cu/54.0	436.50	1.812	-2.199	69	0	--
TACHP-13	Cl	1110±7	0.86	95.2	454.18	3.341	-1.649	161	0	--
TACHP-14	Cl	955±1	1.01	90.1	468.98	2.926	-1.562	265	0	--
TACHP-15	Cl	1085±4	0.97	89.6	440.92	2.976	-1.507	167	0	--
TACHP-16	Cl	483	0.64	87.0	470.17	2.274	-2.106	66	0	--
Tac	-	> 1000	0.30	11.0	198.12	-	-	-	-	-

^a Predicted values using program QikProp v. 2.5[55]; ^b Capacity to scavenge the stable free radical 2,2-diphenyl-1-picrylhydrazyl (DPPH) was monitored according to the Blois method [58] (see **Section 4.4**) (means of two experiments)(EC₅₀, μM); ^c AChE from electric eel, IC₅₀, inhibitor concentration (means of two experiments) for 50% inactivation of AChE; ^d Inhibition of self-mediated A β ₄₂ aggregation (means of two experiments). The Thioflavin-T fluorescence method was used, and the measurements were carried out in the presence of an inhibitor; ^e Assays performed with C_L = 80 μM; *Not determined; ^f Calculated octanol/water partition coefficient; ^g Brain/blood partition coefficient.



Comp	TACHP-9	TACHP-10	TACHP-11	TACHP-12	TACHP-13	TACHP-14	TACHP-15	TACHP-16
R ₁	H	H	H	H	Cl	Cl	Cl	Cl
n	3	4	2	3	3	4	2	3
R	H	H	H	OH	H	H	H	OH

Scheme 16. Representation of TACHP derivatives

4.4 Physicochemical studies

4.4.1 Antioxidant activity

In the herein performed radical scavenging assay with 2,2-diphenyl-1-picrylhydrazyl (DPPH), the TAC-BTA hybrids showed poor antioxidant activity, as already found for tacrine ($EC_{50} > 1000 \mu\text{M}$). All the compounds of this series, apart from **RSC-1**, presented solubility problems in the solvent methanol, compounds **RSC-3**, **4** and **5** being particularly insoluble. **Table 1**, includes the results obtained for compounds **RSC-1**, **2** and **6** ($EC_{50} > 1500 \mu\text{M}$), therefore confirming their low radical scavenging activity.

On the other hand, by analysis of the results contained in **Table 2**, for the TACHP hybrids, it is possible to conclude that some compounds, i.e. **TACHP-9**, **TACHP-10**, **TACHP-12** and **TACHP-16** (EC_{50} ca 399-483 μM), exhibit significant antioxidant activities. These values can be explained mainly by the presence of phenolic hydroxyl groups that are important in the scavenging action of ROS species, although the chain length of the carbon linker connecting both moieties may also play some unexpected role. For instance, **TACHP-9**, with three carbon chain linker and phenolic hydroxyl, shows moderate antioxidant activity ($EC_{50} = 925 \pm 8 \mu\text{M}$), while **TACHP-10** ($EC_{50} = 450 \pm 8 \mu\text{M}$), with four carbon chain linker and phenolic hydroxyl group has a higher scavenging potential. Moving to **TACHP-11**, with two carbon chain linker, i.e. ethyl linker, and also phenolic hydroxyl substitution, the condition becomes very worst ($EC_{50} > 1200 \mu\text{M}$). In **TACHP-12**, another hydroxyl substitution in the three carbon chain linker is present, besides the phenolic hydroxyl of the HP moiety, which enhances the antioxidant capacity significantly ($EC_{50} = 399 \pm 5 \mu\text{M}$). Compounds **TACHP-13** ($EC_{50} = 1110 \pm 7 \mu\text{M}$), **TACHP-14** ($EC_{50} = 955 \pm 1 \mu\text{M}$) and **TACHP-15** ($EC_{50} = 1085 \pm 4 \mu\text{M}$) have chloro substitution on the phenyl ring of the TAC moiety, and this chloro substitution seems to be associated to the decrease of the antioxidant activity of these hybrids with two, three and four carbon chain linkers although the compound with four carbon atoms in the linker **TACHP-14** is slightly better, as already observed for the triad **TACHP-9**, **10** and **11**. Particularly interesting is the fact that **TACHP-16**, containing both hydroxy in a three carbon linker and chloro-substituted TAC, is able to keep a good antioxidant activity ($EC_{50} = 483 \pm 1 \mu\text{M}$).

So, in conclusion, TACHP compounds with extra hydroxyl substituted three carbon chain linkers connecting TAC and HP moieties along with phenolic hydroxyl at the pyridinone ring and with or without chloro-substitution, were found to be good antioxidant compounds (**TACHP-12** $EC_{50} = 399 \pm 5 \mu\text{M}$, **TACHP-16** $EC_{50} = 483 \pm 1 \mu\text{M}$). So hydroxyl substituent increases scavenging capacity by providing a proton to interact with the 2,2-diphenyl-1-picrylhydrazyl (DPPH) free radical, so these compounds able to neutralize free radicals and ROS species. For the remaining compounds of the TACHP series with phenolic hydroxyl a four carbon chain linker seems to privilege better results.

4.4.2 Metal chelation

Some transition metals, such as iron, copper and zinc, have functional roles in the body i.e. these metals can be the co-factors of several enzymes, catalyzing oxidation-reduction reactions, but also it has been proved that metal ions accumulate in the brain with aging leading to oxidative stress and inflammation in the central nervous system (CNS). These symptoms are associated to Wilson's

disease and Alzheimer's disease (AD). Specifically in the case of AD, it is known that iron, copper and zinc deposition in brain leads to metal ion induced A β deposition, while deregulated redox-active metal ions (Cu and Fe) stimulate the overproduction of ROS species with consequent biomolecule degradation. In the present study, the compounds of TACHP series can act as metal chelator, through their HP moiety, and therefore interfere with the above mentioned processes reducing neurotoxicity.

TACHP-12 was the compound chosen as a model for analyzing the chelating capacity of the TACHP hybrids and the equilibrium solution studies were performed in a mixed 20% (w/w) DMSO/water medium, due to solubility reasons. The solvent DMSO was selected because it is quite used and well tolerated in biological and cellular studies.

First, the acid-base behavior of **TACHP-12** was studied, namely its protonation constants ($\log K_i$) were determined by pH-potentiometry (see **Figure 5**). The compound was obtained in the neutral monoprotinated form (HL) and the values of the protonation constants, calculated by fitting the titration experimental curves with Hyperquad 2008 program [60], are contained in **Table 3**. They correspond to the protonation of the phenolic hydroxyl group of the HP moiety (10.54), the TAC amine (8.59) and the pyridinic nitrogen (2.88). In fact, the values of $\log K_1$ and $\log K_3$ of **TACHP-12** are similar to those corresponding to the drug Deferiprone (DFP, $\log K_1$ and $\log K_2$) apart from the different media used for the respective determination.

The chelating capacity of compound **TACHP-12** towards Cu(II) and Zn(II) was evaluated through the determination of the global formation constants of the complexes by pH-potentiometric (Hyperquad 2008 program) [60] titrations while for the Fe(III) complexes by UV-vis spectrophotometry (PSEQUAD program) [61].

All the curves for the Cu/**TACHP-12** and Zn/**TACHP-12** systems lie below that of the ligand for $-2 < a < 1$. This indicates formation of metal complexes with the protonated (in amine tacrine) and deprotonated forms of the ligand with relative stability order Cu(II) > Zn(II), as shown in **Figure 5**, and confirmed by the global stability constants of the respective complexes (see **Table 3**).

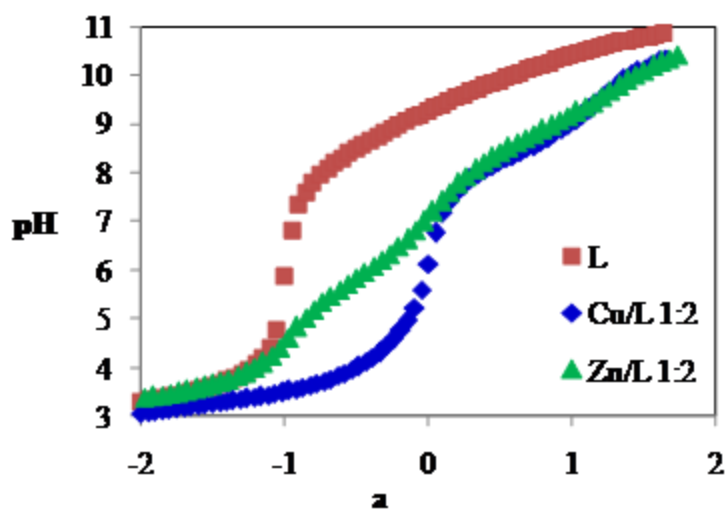


Figure 5. Potentiometric titration curves of **TACHP-12** (20% w/w DMSO/H₂O, $I = 0.1$ M KCl, $T = 25.0 \pm 0.1$ °C, $C_L = 2 \times 10^{-4}$ M); **a** represents moles of base per mole of ligand

In the case of the Fe(III)/**TACHP-12** system, spectrophotometric titrations were performed for the 1:1 and 1:3 Fe(III)/ligand molar ratios because at pH = 2 a high percent of FeHL complex (ca 60%) was already formed. (**Figure 6a**) confirms the consecutive formation of Fe(III) complexes with increasing coordination number, when the pH value increases, since λ_{\max} shifts to lower values. In fact, similar changes in the absorption spectra with the pH were already found for the Fe(III)/DFP [62, 63], which precludes the formation of complexes with the same coordination sphere, involving the two oxygen atoms of the HP moiety.

From the spectra obtained for the 1:1 Fe(III)/**TACHP-12** system, β_{FeHL} was calculated and the stability constants of the remaining complex species, i.e. $\beta_{\text{FeH}_2\text{L}_2}$, $\beta_{\text{FeH}_3\text{L}_3}$ and $\beta_{\text{FeH}_3\text{L}_2}$, were determined from the titration performed under 1:3 molar stoichiometric metal ion to ligand ratio while holding the value of β_{FeHL} constant. (**Figure 6b**) shows the species distribution curves for the 1:3 Fe(III)/**TACHP-12** system where it can be confirmed that the iron complexation started below pH 2, with the formation of both FeHL and FeH₂L₂ complexes, while the fully coordinated tris-chelate species FeH₃L₃ is predominant above pH ca 3.8 and at the physiological pH (7.4) the hexaco-ordinated species FeH₂L₃, with one of the tacrine amines deprotonated, exists in ca 90%. Moreover, by analyzing data contained in **Table 3**, in particular the pFe value at pH 7.4 (21.7) of **TACHP-12**, it is possible to conclude that the studied compound is a quite potent iron chelator, such as the drug DFP (pM ca 19.4 - 20.7 at pH 7.4 in water medium) [62, 63].

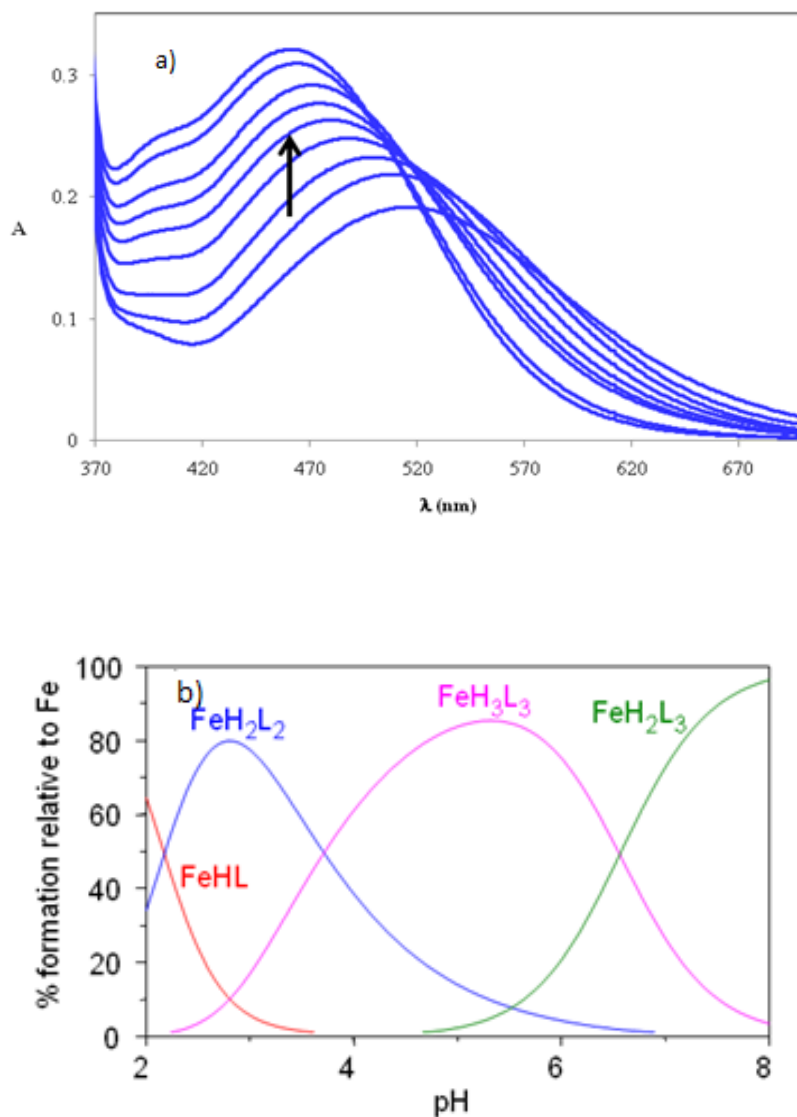


Figure 6. a) Electronic spectra for the 1:3 Fe(III)/TACHP-12 system ($C_L = 2.0 \times 10^{-4}$ M, pH 2.42-7.43); b) Species distribution curves for the 1:3 Fe(III)/TACHP-12 system ($C_L = 2.0 \times 10^{-4}$ M).

In the case of the Cu(II)/TACHP-12 system, both pH-potentiometric titrations were performed for the 1:1 and 1:2 Cu(II)/ligand molar ratios and (Figure 7.) presents the species distribution curves for the 1:2 Cu(II)/L system in the used experimental conditions. In this system, complex formation occurs above pH 2 with the formation of CuHL while the tetradentate species CuH₂L₂ is predominant above pH ca 4 and attains almost 100% formation at the physiological pH. Once again, Table 3, shows a calculated pCu value at pH 7.4 for TACHP-12 (10.8) similar to that of DFP (pM =10.5 at pH 7.4 in water medium [62, 63]), confirming once more the analogous coordination core of both compounds.

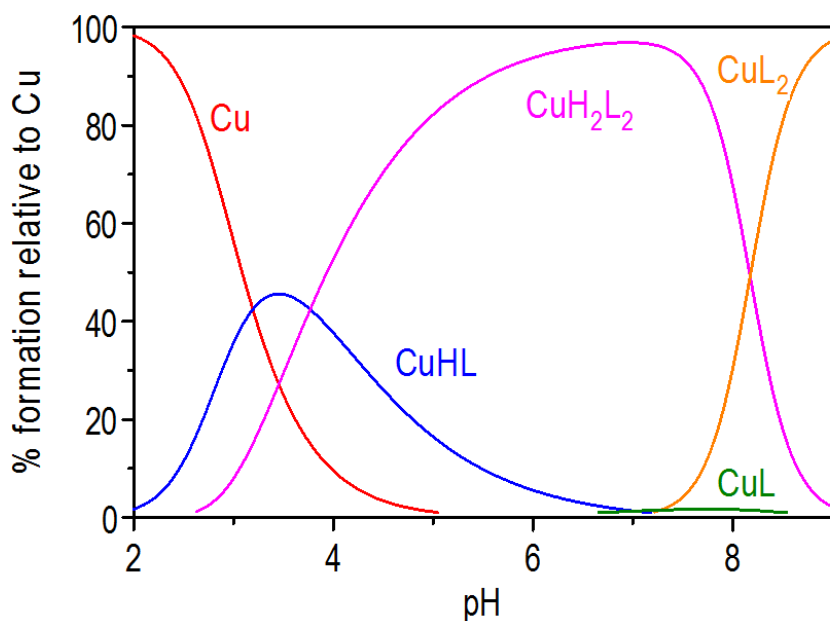


Figure 7. Species distribution curves for the 1:2 Cu(II)/TACHP-12 system ($C_L = 6.7 \times 10^{-4}$ M).

In the case of the Zn(II)/TACHP-12 system, pH-potentiometric titrations were also performed for the 1:1 and 1:2 Zn(II)/ligand molar ratios and the complexation model obtained is presented in **Table 3**, and used in **Figure 8**. In this case, the zinc complexes are weaker, and begin to form only above pH 3.5, which is compatible with the superimposition of the curves of the ligand and Zn/L for $-2 < a < -1$ in **Figure 8**. For $5 < \text{pH} < 8$, a polynuclear Zn_3L_2 species is present but at the physiological pH the 1:1 ZnL complex predominates. The Zn_3L_2 complex probably involves two bidentate coordination of two Zn(II) at the HP moieties plus a tetradentate 4N coordination involving the TAC amine and the N-amide of each ligand with the formation of two 6-chelate rings. Data depicted in **Table 5**, concerning the Zn(II)/TACHP-12 system, shows, once more, a pZn value at pH 7.4 similar to the one found for DFP [62, 63] in water medium.

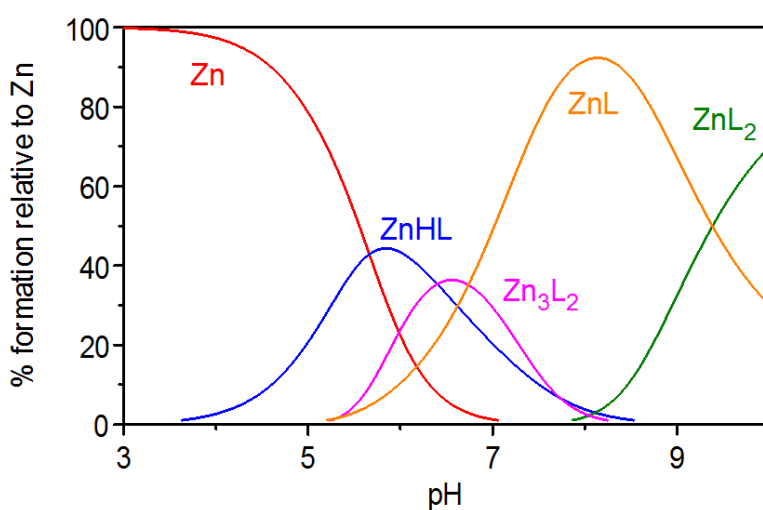
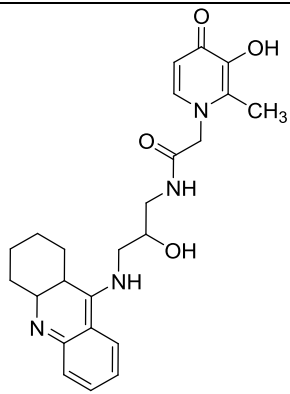
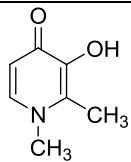


Figure 8. Species distribution curves for the 1:2 Zn(II)/TACHP-12 system ($C_L = 6.7 \times 10^{-4}$ M).

Table 3. Stepwise protonation constants of **TACHP-12**, global formation constants^a of its Fe(III), Cu(II) and Zn(II) complexes ($T = 25.0 \pm 0.1$ °C, $I = 0.1$ M KCl, 20% w/w DMSO/water) and pM^b values

Compounds	$M_mH_hL_l$ (MHL)	$\log K_i$	\log $\beta_{Fe_mH_hL_l}$	\log $\beta_{Cu_mH_hL_l}$	\log $\beta_{Zn_mH_hL_l}$
 <p>TACHP-12</p>	(011)	10.54(5)			
	(021)	8.59(7)			
	(031)	2.88(9)			
	(111)		23.88(5)	19.48(7)	16.78(2)
	(101)		-	12.46(5)	10.16(2)
	(122)		45.62(1)	38.51(6)	-
	(102)		-	22.16(7)	15.18(7)
	(133)		65.57(2)	-	-
	(123)		59.01(4)	-	-
	(302)		-	-	28.79(4)
	pM (pH 7.4)		21.7	10.8	6.9
 <p>DFP^[62, 63]</p>	(011)	9.77 ^[64]			
	(021)	9.82 ^[65]			
		3.62 ^[64]			
		3.66 ^[65]			
	pM (pH 7.4)		19.4; 20.7	10.5	6.3

^a $\beta_{M_mH_hL_l} = [M_mH_hL_l]/[M]^m[H]^h[L]^l$; ^b pM = $-\log[M]$ with $C_L/C_M = 10$ and $C_M = 10^{-6}$ M; ^c .

5. Conclusion

As we know that Alzheimer's disease is of multifactorial nature, so drug development for this disease should take in consideration that drug should be able to modulate multiple targets to improve its efficacy. Thus, compounds as potential drug candidates should have capability to reduce oxidative stress by scavenging free radical, and also should have some structural characteristics that makes it capable to inhibit AChE as well as to reduce the beta aggregation. In the present study some tacrine derivatives i.e. tacrine-methoxyphenylbenzothiazole (BTA) hybrids (**RSC-1** to **RSC-6**) and tacrine-hydroxypyridones (TACHP) hybrids (**TACHP-9** to **TACHP-16**) has been assessed for the antioxidant properties, AChE inhibition, A β self-induced aggregation, in order to evaluate their capacity to combat the main pathophysiological hallmarks of the Alzheimer's disease i.e. oxidative stress, lack of acetylcholine and amyloid plaques of beta amyloid aggregation. Results from the study of these synthetic compounds shows that the BTA hybrids are poor antioxidant but very good AChE inhibitor (even better than the reference tacrine), specifically the chloro derivatives (**RSC-2,4,5**); this behavior is rationalized by the molecular modeling study of all compound, in which the chloro-derivatives proved to interact better with the catalytic triad of AChE. Although beta amyloid studies are not very much conclusive due to the poor solubility of BTA hybrids but seems to possesses good inhibitory activity on self-induced A β_{1-42} aggregation (**RSC-1, 2,3,6** showed the best results). In case of TACHP hybrids, it was observed a moderate antioxidant activity; compounds with OH substitution in linker (**TACHP-10,12,16**) are much better than the reference compound tacrine, while chloro-derivatives(**TACHP-13, 14, and 15**) proved poor antioxidant. TACHP hybrids are conclusive to be good AChE inhibitors, specifically the chloro derivatives of TACHP (**TACHP-12,13,15,16**) but not better than tacrine. From beta amyloid studies it has been concluded that compounds of the TACHP series are very potent inhibitors of self-induced A β_{1-42} aggregation (**TACHP-9** to **16**), even in the presence of copper metal (**TACHP-9** and **12**) inhibited A β_{1-42} aggregation with high potency. Rationalization of these A β_{1-42} aggregation inhibitory results was done through transmission electron microscopy (TEM) assays with model compound **TACHP-12**. It was observed the presence of heavily intertwined networks, for A β_{1-42} alone and in the co-presence of copper, while in the co-presence of ligand **TACHP-12** the aggregates became sparser. Furthermore, 3,4-HP-based chelator **TACHP-12** proved to be a good chelator of Fe, Cu and moderate chelator of Zn, so the potentiometric chelation study of TACHP derivative **TACHP-12** gives support to the potential interest of this chelator in detoxification of hard metal ions, and this is the another promising factor of TACHP series towards the cure of AD.

Overall, these two series of multifunctional tacrine derivatives evidenced several important properties, which make these compounds to deserve future studies for the development of drug candidates against AD.

6. Experimental part

6.1 Chemistry

6.1.1 General Methods and Materials

Analytical grade reagents were purchased from Sigma-Aldrich, Fluka and Acros and were used as supplied. Solvents were dried according to standard methods [66]. The chemical reactions were monitored by TLC using alumina plates coated with silica gel 60 F254 (Merck). Column chromatography separations were performed on silica gel Merck 230-400 mesh (Geduran Si 60). The melting points were measured with a Leica Galen III hot stage apparatus. The ^1H and ^{13}C NMR spectra were recorded on Bruker AVANCE III spectrometers at 300 MHz and 400 MHz, respectively. Chemical shifts (δ) are reported in ppm from the standard internal reference tetramethylsilane (TMS). The following abbreviations are used: s = singlet, d = doublet, t = triplet, m = multiplet. Mass spectra (ESI-MS) were performed on a 500MS LC Ion Trap (Varian Inc., Palo Alto, CA, USA) mass spectrometer equipped with an ESI ion source, operated in the positive ion mode. For the target compounds, the elemental analyses were performed on a Fisons EA1108 CHNS/O instrument and were within the limit of $\pm 0.4\%$.

6.1.2 Experimental Procedure

Synthesis of 3-(benzyloxy)-2-methyl-4*H*-pyran-4-one (**2**):

To a solution of maltol (**1**) (30 g, 0.237 mol) in methanol (100 mL) was added NaOH solution (10.46 g in 30 mL of H_2O), drop wise with stirring. When mixture becomes clear solution then BnCl (26.99 g, 0.213 mol) was added drop wise over a period of 0.5 h and reaction mixture was heated for 12 h. The reaction mixture was cooled to room temperature, filtered to remove the inorganic salt, and the filtrate so obtained was concentrated under reduced pressure. The crude mixture was taken in CH_2Cl_2 (300 mL), and washed with 5% NaOH (2 \times 100 mL) to remove the excess of maltol. The organic layer was washed with brine and dried over anhydrous sodium sulphate and finally evaporated to give the desired compound as an oily material with 82% yield; ^1H NMR (400 MHz, MeOD-d_4), δ (ppm): 2.14 (s, 3H, CH_3), 5.10 (s, 2H, OCH_2Ph), 6.43 (d, 1H, $J = 7.0$ Hz, H-5, Py), 7.37–7.44 (m, 5H, Ph), 7.93 (d, 1H, $J = 8.5$ Hz, H-6, Py); ^{13}C NMR (400 MHz, MeOD-d_4), δ (ppm): 13.68, 73.38, 116.14, 128.15, 128.79, 136.78, 143.46, 155.16, 161.21, 175.98; m/z (ESI MS): calculated for $\text{C}_{13}\text{H}_{12}\text{O}_3$ obtained 239.13 ($\text{M} + \text{Na}$) $^+$.

3-(benzyloxy)-2-methylpyridin-4(1*H*)-one (**3**):

The solution of compound (**2**) (10 g) in ethanol (30 mL) was heated to reflux with 30 mL of 30% aqueous ammonia. After 4 h, during the reflux course, an additional 10 mL of aqueous ammonia was added drop wise with the help of a dropping funnel. The reaction was monitored on TLC, and subjected to completion over a period of 18 h by adding more aqueous ammonia (additional aqueous ammonia is required to add due to its high volatile nature). On completion, the mixture was concentrated under reduced pressure to yield a light brown solid residue, which was recrystallized from ethanol/ether to afford white solid in 80% yield; m.p. 189-190 $^\circ\text{C}$; ^1H NMR (400 MHz, MeOD-d_4),

δ (ppm): 2.08 (s, 3H, CH₃), 5.08 (s, 2H, OCH₂Ph), 6.47 (d, 1H, $J = 7.1$ Hz, H-5, Py), 7.31-7.40 (m, 5H, Ph), 7.54 (d, 1H, $J = 8.0$ Hz, H-6, Py); ¹³C NMR (400 MHz, MeOD-d₄), δ (ppm): 12.85, 72.97, 115.98, 127.91, 128.02, 128.72, 135.01, 137.29, 141.97, 144.82, 174.73; m/z (ESI MS): calculated for C₁₃H₁₃NO₂ obtained 216.05 (M + H)⁺.

Ethyl 2-(3-(benzyloxy)-2-methyl-4-oxopyridin-1(4H)-yl) acetate (4):

The mixture of 3-(benzyloxy)-2-methylpyridin-4(1H)-one (8 g) (37.2 mmol), K₂CO₃ (1 g, 7.3 mmol) in anhydrous DMF (10 mL), was treated with ethyl chloroacetate (1.2 g, 7.3 mmol) and the reaction mixture was stirred for 12 h at room temperature. Progress of reaction was analyzed with the help of TLC. On completion, inorganic material was filtered and the filtrate so obtained was dried under reduced pressure to give a semisolid mixture, which was taken into ethyl acetate and washed with brine solution and water. Finally organic layer was dried over anhydrous sodium sulphate and then evaporated under reduced pressure. The solid material so obtained was washed with diethyl ether to give pure compound (**4**) in 63% yields; m.p. 110-112 °C; ¹H NMR (400 MHz, DMSO-d₆), δ (ppm): 1.05 (m, 3H, CH₃), 1.92 (s, 3H, CH₃), 4.00 (q, 2H, $J = 7.0$ Hz, CH₂CH₃), 4.76 (s, 2H, NCH₂), 4.89 (s, 2H, OCH₂Ph), 6.06 (d, 1H, $J = 10.0$ Hz, 5-HPy), 7.17-7.28 (m, 5H, Ph), 7.45 (d, 1H, $J = 10.3$ Hz, 6-HPy); ¹³C NMR (400 MHz, DMSO-d₆), δ (ppm): 12.42, 14.39, 54.24, 62.02, 72.43, 116.38, 128.31, 128.68, 128.89, 138.11, 140.97, 141.76, 145.50, 168.65, 172.89; m/z (ESI MS): calculated for C₁₇H₁₉NO₄ obtained 302.22 (M + H)⁺.

2-(3-(benzyloxy)-2-methyl-4-oxopyridin-1(4H)-yl) acetic acid (5):

To the solution of ethyl-2-(3-(benzyloxy)-2-methyl-4-oxopyridin-1(4H)-yl)acetate (1 g) in methanol (20 mL), sodium hydroxide solution (1.05 eq, in 1 mL of water) was added and reaction was stirred at room temperature for 3-4 h. Completion of reaction was monitored on TLC. On completion, methanol was removed under reduced pressure to give a light brown solid. The solid material so obtained was then dissolved in 10 mL of ice cold water and acidified with conc. HCl (pH \approx 1-2) to give a white solid, which was filtered and washed with 2 mL of water to give the desired compound (**6**) with 80% yield; m.p. 186-188°C; ¹H NMR (400 MHz, DMSO-d₆), δ (ppm): 2.17 (s, 3H, CH₃), 4.97 (s, 2H, CH₂N), 5.06 (s, 2H, OCH₂Ph), 6.59 (d, 1H, $J = 8.5$ Hz, 5-HPy), 7.34-7.44 (m, 5H, Ph), 7.86 (d, 1H, $J = 10.0$ Hz, 6-HPy); ¹³C NMR (400 MHz, DMSO-d₆), δ (ppm): 12.80, 55.29, 73.16, 128.51, 128.77, 128.95, 137.66, 141.88, 144.51, 144.71, 169.53, 170.40; m/z (ESI MS): calculated for C₁₅H₁₅NO₄ obtained 274.15 (M + H)⁺.

General procedure for synthesis of 2-(3-(benzyloxy)-2-methyl-4-oxopyridin-1(4H)-yl)-N-(3-((1,2,3,4-tetrahydroacridin-9-yl)amino)alkyl)acetamide (14-21):

To the mixture of 2-(3-(benzyloxy)-2-methyl-4-oxopyridin-1(4H)-yl)acetic acid (**5**) (0.5 g, 1.83 mmol) in 25 ml of dry DCM, *N*-methylmorpholine (3.66 mmol) was added under nitrogen. Few minutes later, when reaction become clear solution, propylphosphonic anhydride (T3P) solution (2.2 mmol) was added drop wise under nitrogen and reaction was stirred for half an hour. Finally, solution of different amines (**6-13**) (1.83 mmol) in dry DCM was added to it under nitrogen atmosphere and the reaction mixture was stirred at RT for overnight (completion of reaction mixture was monitored with

TLC). On completion of reaction, DCM layer was washed with brine solution and crude reaction mixture was purified through column chromatography over silica in 3-5% MeOH-DCM system to give desired compounds (**14-21**) in 70-89% yield.

2-(3-(Benzyloxy)-2-methyl-4-oxopyridin-1(4H)-yl)-N-(2-((1,2,3,4-tetrahydroacridin-9-yl)amino)ethyl)acetamide (14):

Compound **14** was obtained as a yellow solid at room temperature in 74% isolated yield from the reaction of **6** with **5** by following the general procedure; m.p. 146-148°C; ¹H NMR (400 MHz, DMSO-d₆), δ (ppm): 1.79 (br.s, 4H, H-2 & H-3), 1.94 (s, 3H, CH₃), 2.65 (br.s, 2H, H-1), 3.02 (br.s, 2H, H-4), 3.51-3.52 (m, 2H, H-2'), 3.99-4.01 (m, 2H, H-1'), 4.68 (s, 2H, NCH₂), 4.98 (s, 2H, OCH₂Ph), 6.98 (d, 2H, *J* = 8.5 Hz, H-5''), 7.30-7.51 (m, 5H, Ph), 7.55 (t, 2H, *J* = 7.0 Hz, H-6 & H-7), 7.82-7.86 (m, 2H, H-5 & NH), 8.04 (d, 1H, *J* = 7.3 Hz, H-8), 8.47 (d, 1H, *J* = 9.5 Hz, H-6''), 9.04 (s, 1H, NH); ¹³C NMR (400 MHz, DMSO-d₆), δ (ppm): 12.47, 20.69, 20.76, 21.89, 24.38, 28.35, 47.59, 55.55, 72.46, 111.76, 115.86, 115.95, 119.58, 125.52, 125.64, 128.24, 128.69, 132.98, 138.19, 141.36., 141.99, 145.37, 151.17, 156.27, 168.01, 172.26; m/z (ESI MS): calculated for C₃₀H₃₂N₄O₃ obtained 497.39 (M + H)⁺.

2-(3-(Benzyloxy)-2-methyl-4-oxopyridin-1(4H)-yl)-N-(3-((1,2,3,4-tetrahydroacridin-9-yl)amino)propyl)acetamide (15):

Compound **15** was obtained as a yellow solid at room temperature in 81% isolated yield from the reaction of **7** with **5** by following the general procedure; m.p. 159-160°C; ¹H NMR (300 MHz, DMSO-d₆), δ (ppm): 1.81 (br.s, 4H, H-2 & H-3), 1.88-1.92 (m, 2H, H-2'), 2.00 (s, 3H, CH₃), 2.67 (br.s, 2H, H-1), 3.01 (br.s, 2H, H-4), 3.19 (t, 2H, H-3'), 3.88-3.90 (m, 2H, H-1'), 4.66 (s, 2H, NCH₂), 4.98 (s, 2H, OCH₂Ph), 6.14 (d, 1H, *J* = 10.5 Hz, H-5''), 7.29-7.40 (m, 5H, Ph), 7.55 (t, 2H, H-6 & H-7), 7.83-7.85 (m, 2H, H-5 & NH), 7.99 (d, 1H, *J* = 7.5 Hz, H-8), 8.44 (1H, H-6''), 8.77 (s, 1H, NH); ¹³C NMR (300 MHz, DMSO-d₆), δ (ppm): 12.55, 20.72, 21.92, 24.50, 28.40, 30.25, 36.40, 45.11, 55.51, 72.35, 111.74, 115.99, 116.06, 119.64, 125.53, 128.20, 128.65, 128.71, 132.94, 138.25, 138.35, 141.30, 141.70, 145.48, 151.14, 156.09, 167.16, 172.61; m/z (ESI MS): calculated for C₃₁H₃₄N₄O₃ obtained 511.40 (M + H)⁺.

2-(3-(Benzyloxy)-2-methyl-4-oxopyridin-1(4H)-yl)-N-(4-((1,2,3,4-tetrahydroacridin-9-yl)amino)butyl)acetamide (16):

Compound **16** was obtained as a yellow solid at room temperature in 80% isolated yield from the reaction of **8** with **5** by following the general procedure; m.p. 84-86 °C; ¹H NMR (400 MHz, DMSO-d₆), δ (ppm): 1.45-1.46 (m, 2H, H-2'), 1.54-1.56 (m, 2H, H-3'), 1.80 (m, 4H, H-2 & H-3), 2.02 (s, 3H, CH₃), 2.71 (br.s, 2H, H-1), 2.90-2.91 (m, 2H, H-4), 3.08-3.10 (m, 2H, H-4'), 3.41-3.42 (t, 2H, *J* = 7.1 Hz, H-1'), 4.56 (s, 2H, NCH₂), 5.01 (s, 2H, OCH₂Ph), 5.45 (br.s, 1H, NH (D₂O exchanged)), 6.14 (d, 2H, *J* = 10.0 Hz, H-5''), 7.32-7.42 (m, 6H, Ph & H-7), 7.50-7.52 (m, 2H, H-6 & H-5), 7.72 (d, 1H, *J* = 7.5 Hz, H-8), 8.12 (1H, H-6''), 8.23 (s, 1H, NH (D₂O exchanged)); ¹³C NMR (400 MHz, DMSO-d₆), δ (ppm): 12.43, 22.89, 23.21, 25.58, 26.92, 28.52, 33.93, 48.06, 55.54, 72.34, 116.00, 116.34, 120.71, 123.50, 123.73, 128.20, 128.39, 128.66, 128.71, 138.36, 141.28, 141.49, 145.58, 147.26, 150.75, 158.32, 166.76, 172.63; m/z (ESI MS): calculated for C₃₂H₃₆N₄O₃ obtained 525.43 (M + H)⁺.

2-(3-(Benzyloxy)-2-methyl-4-oxopyridin-1(4H)-yl)-N-(2-((6-chloro-1,2,3,4-tetrahydroacridin-9-yl)amino)ethyl)acetamide (17):

Compound **17** was obtained as a yellow solid at room temperature in 84% isolated yield from the reaction of **9** with **5** by following the general procedure; m.p. 118-120°C; ¹H NMR (400 MHz, DMSO-d₆), δ (ppm): 1.79-1.81 (m, 4H, H-2 & H-3), 1.96 (s, 3H, CH₃), 2.68 (br.s, 2H, H-1), 2.98-2.90 (m, 2H, H-4), 3.34-3.35 (m, 2H, H-2'), 3.54-3.56 (m, 2H, H-1'), 4.56 (s, 2H, NCH₂), 4.99 (s, 2H, OCH₂Ph), 5.66 (br.s, 1H, NH (D₂O exchanged)), 6.14 (d, 2H, *J* = 10.5 Hz, H-5''), 7.31-7.42 (m, 6H, Ph & H-7), 7.47 (d, 1H, *J* = 7.1 Hz, H-8), 7.73 (s, 1H, H-5), 8.13 (d, 1H, *J* = 8.5 Hz, H-6''), 8.37 (s, 1H, NH (D₂O exchanged)); ¹³C NMR (400 MHz, DMSO-d₆), δ (ppm): 12.39, 22.67, 23.00, 25.34, 33.90, 47.91, 55.46, 72.34, 116.06, 116.51, 118.82, 124.02, 125.91, 128.20, 128.67, 128.68, 133.04, 138.34, 141.20, 141.49, 145.56, 147.91, 150.75, 159.72, 167.59, 172.64; m/z (ESI MS): calculated for C₃₀H₃₁ClN₄O₃ obtained 531.36 (M+H)⁺.

2-(3-(benzyloxy)-2-methyl-4-oxopyridin-1(4H)-yl)-N-(3-((6-chloro-1,2,3,4-tetrahydroacridin-9-yl)amino)propyl)acetamide (18):

Compound **18** was obtained as a yellow solid at room temperature in 89% isolated yield from the reaction of **10** with **5** by following the general procedure; m.p.118-120°C; ¹H NMR (400 MHz, DMSO-d₆), δ (ppm): 1.70-1.76 (m, 2H, H-2'), 1.79-1.80 (m, 4H, H-2 & H-3), 2.01 (s, 3H, CH₃), 2.69-2.70 (m, 2H, H-1), 2.88-2.90 (br.s, 2H, H-4), 3.16 (t, 2H, *J* = 7.1 Hz, H-3'), 3.43 (t, 2H, *J* = 7.1 Hz, H-1') , 4.58 (s, 2H, NCH₂), 5.00 (s, 2H, OCH₂Ph), 5.60 (br.s, 1H, NH (D₂O exchanged)), 6.14 (d, 2H, *J* = 10.5 Hz, H-5''), 7.30-7.37 (m, 5H, Ph), 7.42 (d, 1H, *J* = 8.5 Hz, H-7), 7.51 (d, 1H, H-8), 7.73 (d, 1H, *J* = 8.0 Hz, H-8), 8.14 (d, 1H, *J* = 8.5 Hz, H-6''), 8.27 (s, 1H, NH (D₂O exchanged)); ¹³C NMR (400 MHz, DMSO-d₆), δ (ppm): 12.45, 22.74, 23.04, 25.51, 30.92, 33.98, 36.84, 45.83, 55.48, 72.33, 116.03, 116.86, 119.21, 124.03, 125.77, 127.20, 128.19, 128.65, 128.70, 132.96, 138.33, 141.26, 141.50, 145.56, 148.00, 150.86, 159.91, 167.09, 172.63; m/z (ESI MS): calculated for C₃₁H₃₃ClN₄O₃ obtained 545.41 (M + H)⁺.

2-(3-(Benzyloxy)-2-methyl-4-oxopyridin-1(4H)-yl)-N-(4-((6-chloro-1,2,3,4-tetrahydroacridin-9-yl)amino)butyl)acetamide (19):

Compound **19** was obtained as a yellow solid at room temperature in 83% isolated yield from the reaction of **11** with **5** by following the general procedure; m.p. 118-120°C; ¹H NMR (400 MHz, DMSO-d₆), δ (ppm): 1.41-1.46 (m, 2H, H-2'), 1.54-1.57 (m, 2H, H-3'), 1.78-1.80 (m, 4H, H-2 & H-3), 2.01 (s, 3H, CH₃), 2.67-2.68 (br.s, 2H, H-1), 2.87-2.90 (m, 2H, H-4), 3.07-3.08 (m, 2H, H-4'), 3.56 (t, 2H, *J* = 7.0, H-1'), 4.55 (s, 2H, NCH₂), 4.99 (s, 2H, OCH₂Ph), 5.76 (br.s, 1H, NH (D₂O exchanged)), 6.14 (d, 2H, *J* = 10.5 Hz, H-5''), 7.30-7.37 (m, 5H, Ph), 7.41 (d, 1H, *J* = 8.5 Hz, H-7), 7.50 (d, 1H, *J* = 8.0 Hz, H-8), 7.73 (d, 1H, H-8), 8.16 (d, 1H, H-6''), 8.23 (t, 1H, *J* = 4.0 Hz, NH (D₂O exchanged)); ¹³C NMR (400 MHz, DMSO-d₆), δ (ppm): 12.42, 22.55, 22.94, 25.40, 26.83, 28.36, 33.93, 47.93, 55.54, 72.34, 115.99, 116.13, 118.72, 124.04, 126.04, 128.21, 128.66, 128.73, 133.28, 138.29, 141.29, 141.57, 145.54, 147.33, 151.27, 159.23, 166.76, 172.65; m/z (ESI MS): calculated for C₃₂H₃₅ClN₄O₃ obtained 559.57 (M + H)⁺.

2-(3-(Benzyloxy)-2-methyl-4-oxopyridin-1(4H)-yl)-N-(2-hydroxy-3-((1,2,3,4-tetrahydroacridin-9-yl)amino)propyl)acetamide (20):

Compound **20** was obtained as a yellow solid at room temperature in 74% isolated yield from the reaction of **12** with **5** by following the general procedure; m.p. 134-136°C; ¹H NMR (300 MHz, DMSO-d₆), δ (ppm): 1.81 (br.s, 4H, H-2 & H-3), 2.00 (s, 3H, CH₃), 2.71 (br.s, 2H, H-1), 2.93 (br.s, 2H, H-4), 3.21 (br.s, 2H, H-3'), 3.43-3.59 (m, 2H, H-1'), 3.77 (br.s, 1H, H-2'), 4.62 (s, 2H, NCH₂), 4.98 (s, 2H, OCH₂Ph), 5.41 (br.s, 1H, NH (D₂O exchanged)), 5.98 (br.s, 1H, OH (D₂O exchanged)), 6.13 (d, 2H, *J* = 10.1 Hz, H-5''), 7.30-7.42 (m, 6H, Ph & H-7), 7.51 (d, 1H, *J* = 8.0 Hz, H-5), 7.62 (t, 1H, *J* = 8.5 Hz, H-6), 7.78 (d, 1H, H-8), 8.20 (d, 1H, *J* = 8.0 Hz, H-6''), 8.44 (br.s, 1H, NH (D₂O exchanged)); ¹³C NMR (300 MHz, DMSO-d₆), δ (ppm): 12.52, 22.20, 22.74, 24.83, 32.17, 43.32, 51.87, 55.45, 69.22, 72.34, 115.15, 116.01, 119.20, 124.20, 124.37, 128.20, 128.66, 128.69, 129.94, 138.33, 141.28, 141.54, 145.54, 152.75, 167.46, 172.62; m/z (ESI MS): calculated for C₃₁H₃₄N₄O₄ obtained 527.41 (M + H)⁺.

2-(3-(Benzyloxy)-2-methyl-4-oxopyridin-1(4H)-yl)-N-(3-((6-chloro-1,2,3,4-tetrahydroacridin-9-yl)amino)-2-hydroxypropyl)acetamide (21):

Compound **21** was obtained as a yellow solid at room temperature in 70% isolated yield from the reaction of **13** with **5** by following the general procedure; m.p. 134-136°C; ¹H NMR (400 MHz, DMSO-d₆), δ (ppm): 1.80 (br.s, 4H, H-2 & H-3), 2.00 (s, 3H, CH₃), 2.71 (br.s, 2H, H-1), 2.89 (br.s, 2H, H-4), 3.18 (br.s, 2H, H-3'), 3.32-3.42 (m, 2H, H-1'), 3.70 (br.s, 1H, H-2'), 4.61 (s, 2H, NCH₂), 4.99 (s, 2H, OCH₂Ph), 5.31-5.33 (m, 1H, NH (D₂O exchanged)), 5.36-5.38 (br.s, 1H, OH (D₂O exchanged)), 6.14 (d, 2H, *J* = 10.4 Hz, H-5''), 7.30-7.43 (m, 6H, Ph & H-7), 7.51 (d, 1H, *J* = 7.5 Hz, H-8), 7.73 (s, 1H, H-5), 8.11-8.14 (m, 1H, H-6''), 8.32-8.34 (m, 1H, NH (D₂O exchanged)); ¹³C NMR (400 MHz, DMSO-d₆), δ (ppm): 12.47, 22.74, 23.00, 25.03, 31.13, 43.38, 52.18, 55.48, 69.40, 72.34, 116.02, 116.90, 119.10, 123.99, 125.94, 127.25, 128.18, 128.64, 128.69, 132.94, 138.33, 141.25, 141.51, 145.55, 148.10, 151.07, 159.88, 167.40, 172.63; m/z (ESI MS): calculated for C₃₁H₃₃ClN₄O₄ obtained 561.37 (M + H)⁺.

General procedure for synthesis of 2-(3-hydroxy-2-methyl-4-oxopyridin-1(4H)-yl)-N-(2-((1,2,3,4-tetrahydroacridin-9-yl)amino)alkyl)acetamide (22-29):

The mixture of 2-(3-(benzyloxy)-2-methyl-4-oxopyridin-1(4H)-yl)-N-(3-((1,2,3,4-tetrahydroacridin-9-yl)amino)alkyl)acetamide (**14-21**) (0.95 mmol) and 10% Pd/C in 25 mL of methanol was stirred for 3 h under H₂ (2 bar). Completion of the reaction was monitored on thin layer chromatography (TLC). On completion, reaction mixture was filtered through the bed of celite and evaporated to dryness under reduced pressure to give the desired deprotected 2-(3-hydroxy-2-methyl-4-oxopyridin-1(4H)-yl)-N-(2-((1,2,3,4-tetrahydroacridin-9-yl)amino)alkyl)acetamide derivatives (**22-29**) in 90-95% yield.

2-(3-hydroxy-2-methyl-4-oxopyridin-1(4H)-yl)-N-(2-((1,2,3,4-tetrahydroacridin-9-yl)amino)ethyl)acetamide(22):

Compound **22** was obtained as light yellow solid in 93% yield through the hydrogenolysis of **14** by following general procedure; m.p. 176-177°C; ¹H NMR (400 MHz, DMSO-d₆), δ (ppm): 1.81 (br.s, 4H, H-2 & H-3), 2.00 (s, 3H, CH₃), 2.65 (br.s, 2H, H-1), 3.03 (br.s, 2H, H-4), 3.53 (m, 2H, H-2'), 4.01 (m, 2H, H-1'), 4.68 (s, 2H, NCH₂), 6.10 (d, 2H, *J* = 10.9 Hz, H-5"), 7.48 (d, 1H, *J* = 7.1 Hz, H-5), 7.55 (t, 1H, *J* = 7.5 Hz, H-7), 7.78 (s, 1H, NH (D₂O exchanged)), 7.86 (t, 1H, *J* = 7.5 Hz, H-6), 8.01 (d, 1H, *J* = 7.0 Hz, H-8), 8.46 (d, 1H, H-6"), 8.93 (s, 1H, NH (D₂O exchanged)); ¹³C NMR (400 MHz, DMSO-d₆), δ (ppm): 11.80, 20.77, 21.92, 24.32, 28.48, 31.10, 47.85, 55.54, 110.73, 111.97, 116.09, 119.78, 125.52, 125.60, 129.60, 132.96, 138.54, 139.53, 145.45, 151.38, 156.30, 168.26, 169.69; m/z (ESI MS): calculated for C₂₃H₂₆N₄O₃ obtained 407.38 (M + H)⁺.

2-(3-Hydroxy-2-methyl-4-oxopyridin-1(4H)-yl)-N-(3-((1,2,3,4-tetrahydroacridin-9-yl)amino)propyl)acetamide (23):

Compound **23** was obtained as light yellow solid in 93% yield through the hydrogenolysis of **15** by following general procedure; m.p. 170-172°C; ¹H NMR (400 MHz, DMSO-d₆), δ (ppm): 1.83 (br.s, 4H, H-2 & H-3), 1.92 (br.s, 2H, H-2'), 2.10 (s, 3H, CH₃), 2.69 (br.s, 2H, H-1), 3.03 (br.s, 2H, H-4), 3.21 (br.s, 2H, H-3'), 3.91 (br.s, 2H, H-1'), 4.68 (s, 2H, NCH₂), 6.11 (d, 2H, *J* = 10.9 Hz, H-5"), 7.49-7.51 (m, 1H, H-7), 7.57 (t, 1H, *J* = 7.5 Hz, H-6), 7.84-7.86 (m, 2H, H-5 & NH (D₂O exchanged)), 8.00 (d, 1H, *J* = 7.1 Hz, H-8), 8.45 (1H, *J* = 7.5 Hz, H-6"), 8.72 (s, 1H, NH (D₂O exchanged)), 14.05 (s, 1H, OH (D₂O exchanged)); ¹³C NMR (400 MHz, DMSO-d₆), δ (ppm): 11.95, 20.75, 21.94, 24.52, 28.46, 30.30, 36.42, 45.17, 55.58, 110.73, 111.83, 116.13, 119.73, 125.47, 125.54, 129.67, 132.96, 138.44, 139.52, 145.48, 151.24, 156.12, 167.28, 169.68; m/z (ESI MS): calculated for C₂₄H₂₈N₄O₃ obtained 421.40 (M + H)⁺.

2-(3-hydroxy-2-methyl-4-oxopyridin-1(4H)-yl)-N-(4-((1,2,3,4-tetrahydroacridin-9-yl)amino)butyl)acetamide (24):

Compound **24** was obtained as light yellow solid in 93% yield through the hydrogenolysis of **16** by following general procedure; m.p. 113-114°C; ¹H NMR (400 MHz, DMSO-d₆), δ (ppm): 1.43-1.47 (m, 2H, H-2'), 1.55-1.56 (m, 2H, H-3'), 1.81 (br.s, 4H, H-2 & H-3), 2.10 (s, 3H, CH₃), 2.72 (br.s, 2H, H-1), 2.91 (br.s, 2H, H-4), 3.08-3.10 (m, 2H, H-4'), 3.42 (br.s, 2H, H-1'), 4.60 (s, 2H, NCH₂), 5.45 (br.s, 1H, NH(D₂O exchanged)), 6.10 (d, 2H, *J* = 10.1 Hz, H-5"), 7.35 (t, 1H, *J* = 7.5 Hz, H-7), 7.47 (d, 1H, *J* = 7.1 Hz, H-5), 7.53 (t, 1H, *J* = 7.5 Hz, H-6), 7.72 (d, 1H, *J* = 8.0 Hz, H-8), 8.12 (1H, *J* = 10.9 Hz, H-6"), 8.23 (t, 1H, *J* = 4.0 Hz, NH (D₂O exchanged)); ¹³C NMR (400, MHz, DMSO-d₆), δ (ppm): 11.86, 22.89, 23.21, 25.58, 26.93, 28.52, 33.93, 48.05, 55.59, 110.70, 116.35, 120.71, 123.50, 123.74, 128.39, 128.66, 129.51, 139.54, 145.53, 147.26, 150.75, 158.34, 166.87, 169.78; m/z (ESI MS): calculated for C₂₅H₃₀N₄O₃ obtained 435.46 (M + H)⁺.

N-(2-((6-chloro-1,2,3,4-tetrahydroacridin-9-yl)amino)ethyl)-2-(3-hydroxy-2-methyl-4-oxopyridin-1(4H)-yl)acetamide (25):

Compound **25** was obtained as light yellow solid in 95% yield through the hydrogenolysis of **17** by following general procedure; m.p. 181-182°C; ¹H NMR (400 MHz, MeOD-d₄), δ (ppm): 1.92 (br.s, 4H, H-2 & H-3), 2.18 (s, 3H, CH₃), 2.67 (t, 2H, *J* = 4.0 Hz, H-1), 3.04 (t, 2H, *J* = 4.0 Hz, H-4), 3.74

(br.s, 2H, H-2'), 4.18-4.19 (m, 2H, H-1'), 4.81 (s, 2H, NCH₂), 6.38 (d, 2H, *J* = 10.5 Hz, H-5''), 7.54 (d, 2H, *J* = 7.1 Hz, H-7), 7.59 (t, 1H, *J* = 7.5 Hz, NH (D₂O exchanged)), 7.81 (d, 2H, *J* = 1.5 Hz, H-5), 7.88 (d, 1H, *J* = 7.1 Hz, H-8), 8.44 (d, 1H, *J* = 10.9 Hz, H-6''); ¹³C NMR (400 MHz, DMSO-d₆), δ (ppm): 11.80, 20.77, 21.92, 24.32, 28.48, 31.10, 47.85, 55.54, 110.73, 111.97, 116.09, 119.78, 125.52, 125.60, 129.60, 132.96, 138.54, 139.53, 145.45, 151.38, 156.30, 168.26, 169.69; m/z (ESI MS): calculated for C₂₃H₂₅ClN₄O₃ obtained 441.46 (M + H)⁺.

N-(3-((6-Chloro-1,2,3,4-tetrahydroacridin-9-yl)amino)propyl)-2-(3-hydroxy-2-methyl-4-oxopyridin-1(4H)-yl)acetamide (26):

Compound **26** was obtained as light yellow solid in 92% yield through the hydrogenolysis of **18** by following general procedure; m.p. 162-163°C; ¹H NMR (400 MHz, MeOD-d₄), δ (ppm): 1.98-1.99 (m, 4H, H-2 & H-3), 2.08-2.11 (m, 2H, H-2'), 2.26 (s, 3H, CH₃), 2.76 (br.s, 2H, H-1), 3.04 (br.s, 2H, H-4), 3.45 (t, 2H, *J* = 8.0 Hz, H-3'), 4.03 (t, 2H, *J* = 8.0 Hz, H-1'), 4.79 (s, 2H, NCH₂), 6.40 (d, 2H, *J* = 8.0 Hz, H-5''), 7.53 (d, 1H, *J* = 8.0 Hz, H-7), 7.61 (t, 1H, *J* = 8.0 Hz, NH (D₂O exchanged)), 7.80 (d, 1H, *J* = 8.0 Hz, H-5), 7.88 (d, 1H, *J* = 8.0 Hz, H-8), 8.41 (d, 1H, *J* = 8.0 Hz, H-6''); ¹³C NMR (400 MHz, DMSO-d₆), δ (ppm): 11.96, 20.73, 21.93, 24.52, 28.41, 30.30, 35.42, 45.15, 55.61, 110.75, 111.76, 116.07, 119.64, 125.54, 129.82, 132.97, 138.35, 139.53, 145.45, 151.15, 156.12, 167.27, 169.60; m/z (ESI MS): calculated for C₂₄H₂₇ClN₄O₃ obtained 455.91 (M + H)⁺.

N-(4-((6-chloro-1,2,3,4-tetrahydroacridin-9-yl)amino)butyl)-2-(3-hydroxy-2-methyl-4-oxopyridin-1(4H)-yl)acetamide (27):

Compound **27** was obtained as light yellow solid in 96% yield through the hydrogenolysis of **19** by following general procedure; m.p. 148-149°C; ¹H NMR (400 MHz, MeOD-d₄), δ (ppm): 1.66-1.70 (m, 2H, H-2'), 1.86-1.88 (m, 2H, H-3'), 1.97 (br.s, 4H, H-2 & H-3), 2.27 (s, 3H, CH₃), 2.72 (br.s, 2H, H-1), 3.03 (br.s, 2H, H-4), 3.28-3.30 (m, 2H, H-4'), 4.01 (t, 2H, *J* = 7.0 Hz, H-1'), 4.78 (s, 2H, NCH₂), 6.39 (d, 2H, *J* = 10.5 Hz, H-5''), 7.55 (d, 1H, *J* = 7.5 Hz, H-7), 7.59 (t, 1H, *J* = 8.0 Hz, NH (D₂O exchanged)), 7.78 (d, 1H, *J* = 7.0 Hz, H-5), 7.85 (d, 1H, *J* = 8.5 Hz, H-8), 8.40 (d, 1H, *J* = 10.9 Hz, H-6''); ¹³C NMR (400 MHz, DMSO-d₆), δ (ppm): 11.93, 20.78, 21.97, 24.55, 26.58, 27.84, 28.52, 38.76, 47.24, 55.66, 110.69, 111.73, 116.16, 119.82, 125.47, 129.73, 132.84, 138.54, 139.59, 145.47, 151.32, 155.95, 167.00, 169.67; m/z (ESI MS): calculated for C₂₅H₂₉ClN₄O₃ obtained 470.14 (M + H)⁺.

2-(3-hydroxy-2-methyl-4-oxopyridin-1(4H)-yl)-N-(2-hydroxy-3-((1,2,3,4-tetrahydroacridin-9-yl)amino)propyl)acetamide (28):

Compound **28** was obtained as light yellow solid in 91% yield through the hydrogenolysis of **20** by following general procedure; m.p. 150-152°C; ¹H NMR (400 MHz, DMSO-d₆), δ (ppm): 1.82 (br.s, 4H, H-2 & H-3), 2.09 (s, 3H, CH₃), 2.72 (br.s, 2H, H-1), 2.94 (br.s, 2H, H-4), 3.23 (t, 2H, *J* = 7.0 Hz, H-3'), 3.47-3.49 (m, 1H, Ha-1'), 3.58-3.61 (m, 1H, Hb-1'), 3.79-3.80 (m, 1H, H-2'), 4.67 (s, 2H, NCH₂), 5.99 (br.s, 1H, NH (D₂O exchanged)), 6.10 (d, 2H, *J* = 10.1 Hz, H-5''), 7.41 (t, 1H, *J* = 7.5 Hz, H-7), 7.48 (d, 1H, *J* = 7.1 Hz, H-5), 7.65 (t, 1H, *J* = 7.0 Hz, H-6), 7.79 (d, 1H, *J* = 7.5 Hz, H-8), 8.21 (d, 1H, *J* = 10.5 Hz, H-6''), 8.47 (t, 1H, NH (D₂O exchanged)); ¹³C NMR (400 MHz, DMSO-d₆), δ (ppm): 11.93, 22.21, 22.74, 24.84, 31.09, 43.33, 51.89, 55.52, 69.25, 110.73, 115.18, 119.21, 124.21, 124.38,

125.80, 129.58, 129.94, 139.54, 144.43, 145.49, 152.74, 156.04, 167.58, 169.78; m/z (ESI MS): calculated for C₂₄H₂₈N₄O₄ obtained 437.40 (M + H)⁺.

N-(3-((6-chloro-1,2,3,4-tetrahydroacridin-9-yl)amino)-2-hydroxypropyl)-2-(3-hydroxy-2-methyl-4-oxopyridin-1(4H)-yl)acetamide (29):

Compound **29** was obtained as light yellow solid in 91% yield through the hydrogenolysis of **21** by following general procedure; m.p. 161-162 °C; ¹H NMR (400 MHz, MeOD-d₄), δ (ppm): 1.97-1.98 (br.s, 4H, H-2 & H-3), 2.27 (s, 3H, CH₃), 2.75 (br.s, 2H, H-1), 3.05 (br.s, 2H, H-4), 3.41-3.47 (br.s, 2H, H-3'), 3.91-3.95 (m, 1H, H-1'), 4.0-4.09 (m, 1H, H-2'), 4.80 (s, 2H, NCH₂), 6.37 (d, 2H, *J* = 10.0 Hz, H-5''), 7.50 (d, 1H, *J* = 7.5 Hz, H-7), 7.58 (t, 1H, NH (D₂O exchanged)), 7.78 (d, 1H, *J* = 7.7 Hz, H-5), 7.85 (d, 1H, *J* = 8.5 Hz, H-8), 8.43 (d, 1H, *J* = 10.5 Hz, H-6''); ¹³C NMR (400 MHz, DMSO-d₆), δ (ppm): 12.00, 20.84, 21.94, 24.37, 28.61, 43.19, 51.25, 55.56, 68.86, 110.75, 112.13, 116.34, 119.96, 125.40, 125.53, 129.72, 132.83, 138.70, 139.55, 145.46, 151.48, 156.35, 167.61, 169.73; m/z (ESI MS): calculated for C₂₄H₂₇ClN₄O₄ obtained 471.84 (M + H)⁺.

6.2 Biological activities

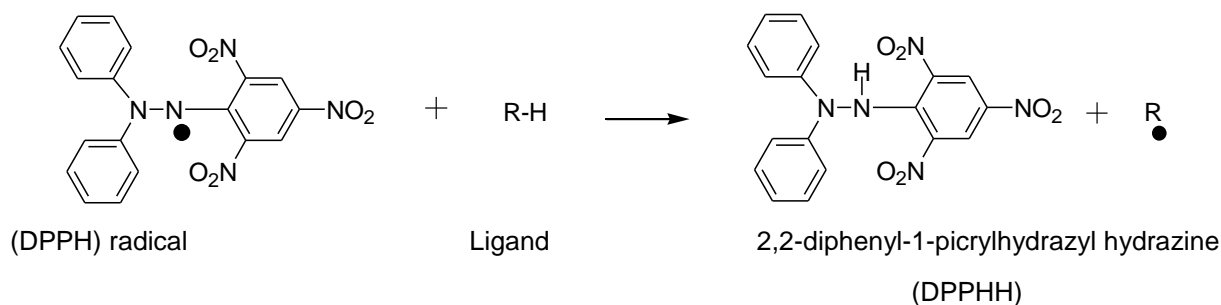
6.2.1. Material and equipment

Analytical grade reagents and solvents were purchased from Sigma-Aldrich, Fluka and Acros and were used as supplied. For antioxidant assay reading the solution absorbance at 517 nm, recorded on a Perkin-Elmer scan Lambda 35 UV-Vis Spectrophotometer. For AChE inhibition the initial rate of the enzymatic reaction was monitored by reading the solution absorbance at 405 nm, recorded on a Perkin-Elmer Lambda 35 UV-Vis spectrophotometer. ThT fluorescence assay for β-amyloid aggregation was measured using a Cary Eclipse of Varian fluorimeter. (Molecular Devices) at the following wavelengths: excitation (446 nm) and emission (486 nm). TEM assays were performed with a Hitachi H8100 transmission electron microscope, at MicroLab/IST. Amyloid β-peptide, (1-42) (Aβ₁₋₄₂), was purchased from Aldrich as a lyophilized powder.

6.2.2. Anti-oxidant activity

All synthesized ligands were investigated for their antioxidant activity (EC₅₀), based on reduction of 2,2-diphenyl-1-picrylhydrazyl (DPPH), a stable free radical. The free radical DPPH with an odd electron having purple color gives a maximum absorption at 517 nm [67, 58]. When an antioxidant (synthetic ligand) reacts with DPPH, which is a stable free radical, it becomes paired off in the presence of hydrogen donor (i.e. free radical scavenging antioxidant ligand) and 2,2-diphenyl-1-picrylhydrazyl (DPPH) reduced to 2,2-diphenyl-1-picrylhydrazyl-hydrazine (DPPHH) and so absorbance decreased from DPPH radical to DPPHH form which results in the decolorisation of purple color to yellow color. So this antioxidant assay by DPPH method is the most accepted model for evaluating the free radical scavenging activity of any new drug. Compounds that can donate hydrogen atoms to DPPH are able to give rise to the reduced form of DPPHH and in that case the violet color

changes to the pale yellow color from the picryl group. In the presence of any free radical scavenger, this odd electron pairs up and causes the diminishing of absorption band which is proportional to the number of electrons taken up.



Scheme 17. Reaction of 2,2-diphenyl-1-picrylhydrazyl (DPPH) radical with hydrogen donating ligand to give 2,2-diphenyl-1-picrylhydrazyl hydrazine (DPPHH)

The capacity to scavenge the stable free radical 2,2-diphenyl-1-picrylhydrazyl (DPPH) was monitored according to the Blois method [58] by reading the solution absorbance at 517 nm, recorded on a Perkin-Elmer scan Lambda 35 UV-Vis Spectrophotometer. The test compounds (200 μ L-1 mL) were mixed with 2.5 mL of DPPH solution and filled up with methanol solvent to the total volume of 3.5 mL according to **Table 4**. The samples were incubated for 30 min at room temperature protected from light. The absorbance was measured at 517 nm against the corresponding blank (methanol) in a visible range (300-700 nm) of spectrophotometer. The antioxidant activity was calculated by an equation shown in **Annexure 1**. The compound antioxidant activity (EC_{50}) was obtained by plotting the antioxidant activity against the compound concentration.

Table 4. Solution preparation for antioxidant assay

^a $V_T = 3.5$ mL

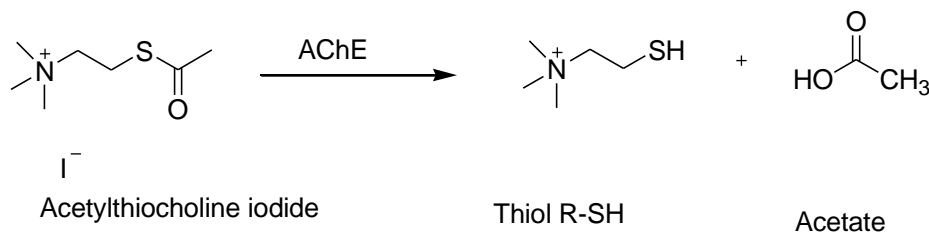
Solution	1	2	3	4	5	6
DPPH	2.5mL	2.5 mL	2.5 mL	2.5 MI	2.5mL	2.5mL
MeOH	1mL	800 μ L	600 μ L	400 μ L	200 μ L	0
Inhibitor	0 mL	200 μ L	400 μ L	600 μ L	800 μ L	1 mL

^aTotal volume of each solution

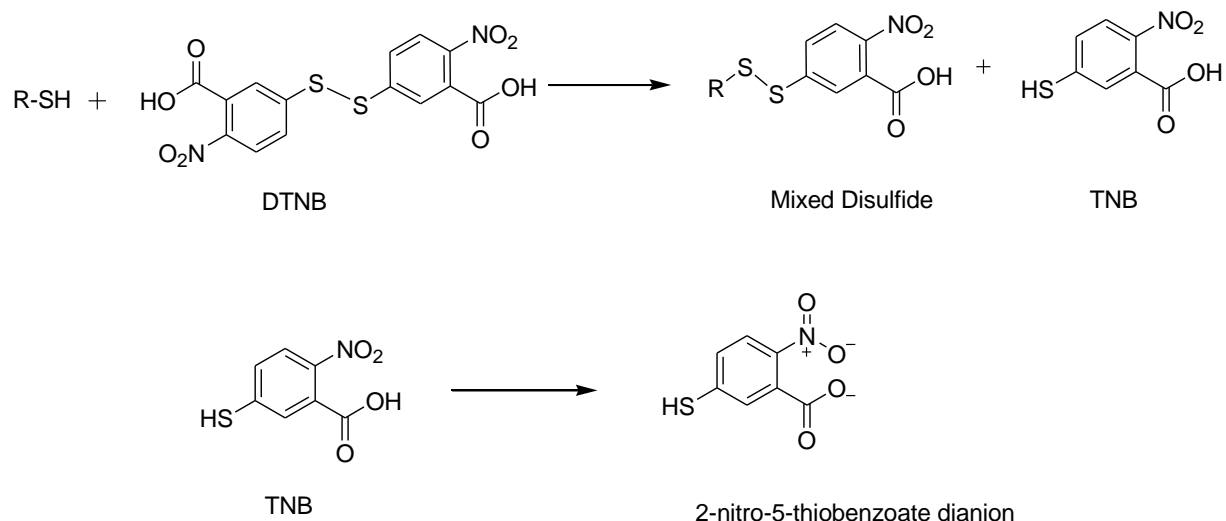
6.2.3. Acetylcholinesterase Activity Assay

This assay is mainly dealing with the evaluation of the inhibitory potential of the compounds. So AChE inhibitors are among the key drugs approved for Alzheimer's disease (AD) [68]. Assay of acetylcholinesterase activity carried out with Acetylcholinesterase stock solution was prepared by dissolving 500 U (extracted from *Electrophorus electricus* and purchased from Sigma-Aldrich) in TRIS buffer (50 mM, pH 8) (10 mL). The enzyme was later diluted with HEPES buffer to give the final AChE concentration conditions [69]. The initial rate of the enzymatic reaction was monitored by reading the solution absorbance at 405 nm, recorded on a Perkin-Elmer Lambda 35 UV-Vis Spectrophotometer. In this modification method of Ellman *et al.* [43, 52, 68] used for the determination of AChE activity, portions of enzyme were added to HEPES buffer and in different volume inhibitor and methanol were added to it then samples were left to incubate for 15 min at room temperature then sodium chloride and magnesium chloride, pH 8.0, containing 5,5'-dithiobis(2-nitrobenzoic acid) (DTNB) and acetylthiocholine iodide (AChI) i.e. the substrate for enzyme and source of thiol also added to it and reaction was monitored for 5 min at 405 nm. All the solutions were prepared according to **Table 5**. Also run with a blank containing all the components except AChE, which was replaced by HEPES buffer. The velocities of the reaction were calculated as well as the enzyme activity. A control reaction was carried out using the sample solvent (methanol) in the absence of any tested compound, and it was considered as 100% activity. The percentage inhibition of the enzyme activity due to the presence of increasing test compound concentration was calculated by the equation shown in **Annexure 2**. Then percentage inhibition plotted against the concentration of compound from where we can get the IC_{50} value, which gives idea about the inhibitory capacity of compound.

In this method thiol group of the acetylthiocholine iodide reacts with DTNB cleaving the disulfide bond to give 2-nitro-5-thiobenzoate (TNB), which ionizes to the TNB^{2-} dianion in water at neutral and alkaline pH. This TNB^{2-} ion has a yellow color and this reaction is rapid and stoichiometric, with the addition of one mole of thiol releasing one mole of TNB. The TNB^{2-} is quantified in a spectrophotometer by measuring the absorbance of visible light at 405 nm [69].



Scheme 18. Reaction of AChE with substrate AChE to give thiol (R-SH)



Scheme 19. Reaction of DTNB with a thiol (R-SH)

Table 5. Solution preparation for Acetylcholinesterase Activity Assay

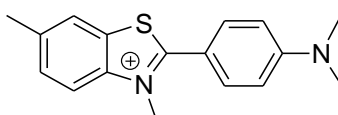
ASSAY		BLANK	
HEPES	374 μL	HEPES	374 μL
AChE	25 μL	HEPES	25 μL
MeOH	(0-40) ^a μL	MeOH	(0-40) ^a μL
INHIBITOR	(10-50) ^b μL	INHIBITOR	(10-50) ^b μL
15 min			
AChI	75 μL	AChI	75 μL
DTNB	476 μL	DTNB	467 μL

^aAmount of methanol varies according to the ^bamount of inhibitor.

6.2.4 Amyloid beta aggregation assay

As we know through genetic and biochemical studies that the formation of β -amyloid ($A\beta$) plaques is a key neurodegenerative event in Alzheimer's disease (AD) and so a logical approach to treat AD is the development of small molecule inhibitors that either blocks the proteases that generate $A\beta$ from its precursor (β - and γ -secretases) or reverse $A\beta$ aggregation. The ThT (Thioflavin T) β -Amyloid aggregation assay provides a convenient and standard method [70] to measure $A\beta_{42}$ aggregation using Thioflavin T dye. $A\beta_{42}$ peptide is pre-treated to ensure that it is in a monomeric

state. An optimized fibrillation buffer i.e. phosphate buffer is included and also a known inhibitors (tacrine) is assayed as control. The assay is based on the property of ThT dye in which fluorescence is increased when bound to aggregated A β peptides, but when a compound, which act as inhibitor of aggregated A β peptides, is added to it the fluorescence intensity decreases [71]. ThT fluorescence was measured using a Cary Eclipse of Varian fluorimeter (molecular Devices) at the following wavelengths: excitation (446 nm) and emission (486 nm). From this intensity difference, it is possible to calculate the percentage inhibition capacity of the compound by using equation shown in **Annexure 3**.



Scheme 20. Structure of Thioflavin -T dye

Table 6. Preparation of solutions for Amyloid beta aggregation inhibition assay.

Control

BLANK	ASSAY
PHOSPHATE BUFFER 60 μ L pH=8	PHOSPHATE BUFFER 30 μ L ^a A β ₄₂ (40 μ M) 30 μ L
After 24 h (immediately before reading in the fluorimeter) 180 μ L ^b ThT (5 μ M) in glycine NaOH buffer.	

Ligand

BLANK	ASSAY
PHOSPHATE BUFFER 50 μ L Ligand (80 μ M) 10 μ L	PHOSPHATE BUFFER 20 μ L Ligand (80 μ M) 10 μ L ^a A β ₄₂ (40 μ M) 30 μ L
After 24 h (immediately before reading in the fluorimeter) 180 μ L ^b ThT (5 μ M) in glycine NaOH buffer.	

^aA β ₁₋₄₂ peptide, ^bThioflavin T dye.

6.2.5 Transmission Electron Microscopy (TEM)

The samples for TEM assays were previously prepared according to the following procedure. A β stock solutions were prepared by dissolving the lyophilized peptide in a mixture of acetonitrile (48

μL), 2% NH_4OH (10 μL) and NaCl 300 μM (48 μL). The peptide stock solution was diluted to a final concentration of 50 μM in a buffered solution containing 4-(2-hydroxyethyl)-1-piperazine-ethanesulfonic acid (HEPES, 50 mM, pH = 6.6). For the inhibition studies, compounds (50 μM final concentration) were added to the sample of $\text{A}\beta$ (25 μM final concentration) in the absence or in the presence of copper chloride (25 μM final concentration) followed by incubation for 24 h at 37 $^\circ\text{C}$. Formvar/Carbon 200-mesh Cu grids (Ted Pella) were treated with amyloid- β peptide aggregated samples (10 μL) for 2 min at room temperature. Excess samples were removed using filter paper followed by washing twice with deionized water. Each grid incubated with uranyl acetate (1%, 10 μL , 1 min) was stained and dried for 15 min at room temperature. Images from each sample were taken by a Hitachi H8100 TEM with a Lab 6 filament (200kV, 10000-20000 \times magnification).

6.2.6 Potentiometric and spectrophotometric studies

pH-potentiometric and UV-Vis spectrophotometric titrations of compound **TACHP-12** were done in a 20% w/w DMSO/ H_2O medium, at $T = 25.0 \pm 0.1$ $^\circ\text{C}$ and ionic strength (I) 0.1 M KCl, by using 0.1 M KOH as titrant.

Both glass and Ag/AgCl reference electrodes were previously calibrated in different DMSO/ H_2O mixtures of increasing DMSO % composition i.e. first with aqueous solution, then 10% and 20% DMSO/ H_2O respectively and the response of the glass electrode was evaluated by strong acid – strong base (HCl/KOH) calibrations with the determination of the Nernst parameters by Gran's method [72]. The measurements were performed in a final volume of 30.00 mL, the ligand concentrations (C_L) were 6.7×10^{-4} M (potentiometry) and 2.0×10^{-4} M (spectrophotometry), under different C_M/C_L ratios: 0:1 (L), 1:1 (M/L, M = Fe, Cu, Zn), 1:2 (M/L, M = Cu, Zn) and 1:3 (M=Fe). The spectrophotometric measurements were carried out in a 300–700 nm wavelength range at pH approximately 2-9.

All titrations were performed in triplicate and under the stated experimental conditions the pK_w value (13.7) was determined and subsequently used in the computations. The stepwise protonation constants of the ligand, $K = [\text{HL}]/[\text{L}][\text{H}]$ and the overall metal–complex stability constants $\beta_{M_mH_hL_l} = [\text{M}_m\text{H}_h\text{L}_l]/[\text{M}]^m[\text{H}]^h[\text{L}]^l$, were calculated by fitting the pH-potentiometric and spectrophotometric data with, respectively, Hyperquad 2008 [60] and PSEQUAD [61] programs. The metal hydrolysis constants were taken from values in the literature [72] determined in aqueous media and were also included in the equilibrium models. The species distribution curves were obtained with the Hyss program [60].

6.2.7 Molecular modeling

The modeling of ligand–protein docking was performed using program GOLD, v. 5.1 [53]. The X-ray crystallographic structure of acetylcholinesterase *Torpedo californica* AChE (*TcAChE*) in complexation with an inhibitor (original ligand) was taken from RCSB Protein Data Bank (PDB entry 1ODC) [54] to be used as a receptor in the docking simulations. For simulations, original complex

structure was treated using a MAESTRO v. 9.3 [56] by removing the original ligand, solvent, and co-crystallization molecules and also by adding hydrogen atoms. The 3D structures of the ligand (synthetic inhibitors) were built with Maestro, first of all geometry of synthetic ligand was optimized by making a random conformational search (RCS) of 1000 cycles, after that optimization done by 2500 optimization steps with a program GHEMICAL v. 2.0 [73]. All ligands were docked into the AChE structure using GOLD v. 5.1 [53] with the default parameters of GOLD and the ASP scoring function. The zone of interest was defined as the residues within 10 Å from the original position of the ligand in the crystal structure.

6.2.8 Pharmacokinetic study

Prediction of some pharmacokinetic proprieties were carried out using *in silico* tools, namely descriptors using QIKPROP v. 2.5 [55] provided by MAESTRO [56]. The following drug-like properties have been calculated: the lipo-hydrophilic character (clog *P*), blood–brain barrier partition coefficient (log BB), the ability to be absorbed through the intestinal tract (Caco-2 cell permeability), and CNS activity along with the verification of Lipinski's rule of five. This study may give an idea of drug likeness of different synthesized hybrid compounds for being orally used as anti-AD agents.

7. References

- [1] Alzheimer's Association, Alzheimer's disease facts and figures, *Alzheimer's Dement.*, vol. 13, pp. 325, 2017.
- [2] Z. Najafia, M. Saeedi, M. Mahdavid, R. Sabourianc, M. Khanavie, B. Tehrania, H. Moghadamf, N. Edrakig, E. Karimpor-Razkenaric, *Bioorg. Chem.*, vol. 67, pp. 84, 2016.
- [3] http://www.alz.org/alzheimers_disease_what_is_alzheimers.asp (accessed February 2017-August 2017).
- [4] A. Nunes, S. M. Marques, C. Quintanova, D. F. Silva, S. M. Cardoso, S. Chaves, M. A. Santos, *Dalton Trans.*, vol. 42, pp. 6058, 2013.
- [5] A. C. Daban, A. Day, P. Faller, C. Hureau, *Dalton Trans.*, vol. 45, pp. 15671, 2016.
- [6] M. R. Jonesa, C. Dyragera, M. Hoaraua, K. J-Korshavn, M. H. Limc, A. Ramamoorthy, T. Storr, *Inorg. Bio. Chem.*, vol. 158, pp. 131, 2016.
- [7] L. R. Santiago, J. A. Torres, P. Vidossich, M. Sodupea, *Phys. Chem. Chem. Phys.*, vol. 17, pp. 13582, 2015.
- [8] A. Kumar, A. Singh, E. Ekavali, *Pharmacol. Rep.*, vol. 67, pp. 195, 2015.
- [9] H. Sies, *Oxidative stress*, edited by Academic press, London, 1985.
- [10] M. Schieber, N. S. Chandel, *Curr. Bio.*, vol. 24, pp. 453, 2014.
- [11] D. Munro, J. R. Treberg, *J. Exp. Bio.*, vol. 220, pp. 1170, 2017.
- [12] S. Reuter, S. C. Gupta, M. M. Chaturvedi, B. B. Aggarwal, *Free Radical Bio. & Med.*, vol. 49, pp. 1603, 2010.
- [13] K. Jomova, M. Valko, *Toxicology*, vol. 283, pp. 65, 2011.
- [14] J. H. Roh, Y. Huang, A. W. Bero, T. Kasten, F. R. Stewart, R. J. Bateman, D. David, *Scienc.Trans. Med.*, vol. 4, pp. 122, 2010.
- [15] A. S. Pithadia, M. H. Lim, *Curr. Opin. Chem. Bio.*, vol. 16, pp. 67, 2012.
- [16] S. H. Omara, C. J. Scotta, A. S. Hamlinc, H. K. Obied, *The J. Nutri. Bio. Chem.*, vol. 47, pp. 20, 2017.
- [17] P. Xu, M. Zhang, R. Sheng, Y. Ma, *Europ. J. Med. Chem.*, vol. 127, pp. 174, 2017.
- [18] O. Obini, E. Gold, G. I. Giac, *Nat. Rev. Neuro.*, vol. 9, pp. 677, 2013.
- [19] H. Dvir, I. Silman, M. Harel, T. L. Rosenberry, J. L. Sussman, *Chemico-Bio. Interact.*, vol. 187, pp. 10, 2010.
- [20] M. P. Goeldner, C. G. Hirth, *Proc. Natl. Acad. Sci. U.S.A.*, vol. 77, pp. 6439, 1980.
- [21] C. de los Rios, *Expert Opin. Ther. Patents.*, vol. 22, pp. 853, 2012.
- [22] M. Goedert, M. G. Spillantini, *Scienc.*, vol. 314, pp. 777, 2006.

- [23] K. William-Summers, M. D., *Feature Art.*, vol. 5, pp. 01, 2000.
- [24] M. A. Santos, K. Chand, S. Chaves, *Coord. Chem. Rev.*, vol. 327, pp. 287, 2016.
- [25] J. C. Soares, S. Gershon, *Pharmacol. Prop.*, vol. 6, pp. 225, 1995.
- [26] C. Quintanova, R. S. Keri, S. M. Marques, M. G-Fernandes, S. M. Cardoso, M. L. Serralheiro, M. A. Santos, *Med. Chem. Commun.*, vol. 6, pp. 1969, 2015.
- [27] M. Kozurkova, S. Hamulakova, Z. Gazova, H. Paulikova, P. Kristian, *Pharmacol.*, vol. 4, pp. 382, 2011.
- [28] M. Racchi, M. Mazzucchelli, E. Porrello, C. Lanni, S. Govoni, *Pharmacol. Res.*, vol. 50, pp. 441, 2004.
- [29] M. C. Rodrigues-Simoes, F. P. Dias-Viegas, M. S. Moreira, M. F. Silva, M. M. Riquiel, P. M. da Rosa, M. R. Castelli, M. H. Dos-Santos, M. G. Soares, C. Viegas, *Mini-Rev. in Med. Chem.*, vol. 14, pp. 2, 2014.
- [30] F. P. D. Viegas, M. C. R. Simoes, M. D. Rocha, M. R. Castelli, M. S. Moreira, C. D. Viegas Junior, *Rev. Virtual Quim.*, vol. 4, pp. 286, 2011.
- [31] K. Kawakami, Y. Inoue, A. Kawai, T. Wakita, M. Sugimoto, H. Hopfinger, *Bioorg. Med. Chem.*, vol. 4, pp. 1429, 1996.
- [32] P. S. Yadav, D. Devprakash, G. P. Senthilkumar, *J. Intern. Pharma. Scienc. and Drug Reseac.*, vol. 3, pp. 01, 2011.
- [33] L. Hroch, L. Aitken, O. Benek, M. Dolezal, K. Kuca, F. G. Moore, K. Musilek, *Curr. Med. Chem.*, vol. 22, pp. 730, 2015.
- [34] M. Ono, S. Hayashi, H. Kimura, H. Kawashima, M. Nakayama, H. Saji, *Bioorg. & Med. Chem.*, vol. 17, pp. 7002, 2009.
- [35] R. Koteswara, V. Valasani, G. Hu, O. Michael, C. Chaney, S. Shirley, *Chem. Biol. Drug Des.*, vol. 81, pp. 238, 2013.
- [36] R. S. Keri, M. R. Patil, S. A. Patil, S. Budagumpi, *Europ. J. Med. Chem.*, vol. 89, pp. 207, 2015.
- [37] M. D. Altintop, Z. A. Kaplancikli, A. Ozdemir, G. T. Zitouni, H. E. Temel, G. Akalin, *Arch. Pharm. Chem. Life Sci.*, vol. 345, pp. 112, 2012.
- [38] H. C. Korting, M. Grundmann- Kollmann, *Mycoses*, vol. 40, pp. 243, 1999.
- [39] L. Zhiliang, Y. Zhang, M. Zhang, H. Chen, Z. Sun, D. Geng, C. Niu, K. Li, *Europ. J. Med. Chem.*, vol. 67, pp. 447, 2013.
- [40] R. Lissette, P. Perez, J. Katherine, F. Franz, *Dalton Trans.*, vol. 39, pp. 2177, 2010.
- [41] W. Huang, W. Wei, Z. Shen, *RSC Adv.*, vol. 94, pp. 01, 2014.
- [42] S. Chaves, L. Piemontese, A. Hiremathad, M. A. Santos, *Curr. Med. Chem.*, vol. 24, 2017. DOI: 10.2174/0929867324666170330092304.

- [43] R. S. Keri, C. Quintanova, S. M. Marques, A. R. Esteves, S. M. Cardoso, M. A. Santos, *Bioorg. & Med. Chem.*, vol. 21, pp. 4559, 2013.
- [44] A. Hiremathad, K. Chand, A. R. Esteves, S. M. Cardoso, R. R. Ramsay, S. Chaves, R. S. Keri, M. A. Santos, *RSC Adv.*, vol. 6, pp. 53519, 2016.
- [45] M. A. Santos, S. Chaves, *Future Med. Chem.*, vol. 7, pp. 383, 2015.
- [46] M. A. Santos, K. Chand, S. Chaves, *Future Med. Chem.*, vol. 8, pp. 2113, 2016.
- [47] M. Mohammadpour, A. Sadeghi, A. Fassihi, L. Saghaei, A. Movahedian, M. Rostami, *J. Pharm. Scienc.*, vol. 7, pp. 171, 2012.
- [48] K. Chand, H. M. Alsoghier, S. Chaves, M. A. Santos, *J. Inorg. Bio. chem.*, vol. 163, pp. 266, 2016.
- [49] E. David, G. Green, L. Meryn, B. Bowen, E. Lauren, S. Scott, T. Storr, M. Merkel, K. Bohmerle, H. Katherine, T. Thompson, O. Brian, P. Patrick, J. Harvey, S. Schugar, C. Orvig, *Dalton Trans.*, vol. 39, pp. 1604, 2010.
- [50] M. Tonelli, M. Catto, B. Tasso, F. Novelli, C. Canu, G. Iusco, L. Pisani, *Chem. Med. Chem.*, vol. 10, pp. 1040, 2015.
- [51] A. Nunes, S. M. Marques, C. Quintanova, D. F. Silva, S. M. Cardoso, S. Chaves, M. A. Santos. *Dalton Trans.*, vol. 42, pp. 6058, 2013.
- [52] J. Sebestik, S. M. Marques, P. L. Fale, S. Santos, D. M. Arduino, S. M. Cardoso, C. R. Oliveira, M. L. Serralheiro, M. A. Santos, *Enzyme Inhib. Med. Chem.*, vol. 26, pp. 485, 2011.
- [53] G. Jones, P. Willett, R. C. Glen, A. R. Leach, R. Taylor, *J. Mol. Biol.*, vol. 267, pp. 727, 1997.
- [54] Protein Data Base (PDB). <http://www.pdb.org/pdb/home/home.do> (accessed March 2016–July 2017).
- [55] QikProp, version 2.5, Schrödinger, LLC, New York, NY, 2005.
- [56] Maestro, version 9.3, Schrödinger Inc., Portland, OR, 2012.
- [57] C. A. Lipinski, F. Lombardo, B. W. Dominy, P. J. Feeney, *Adv. Drug Delivery Rev.*, vol. 23, pp. 3, 1997.
- [58] M. K. Prashanth, M. Madaiah, H. D. Revanasiddappa, K. N. Amruthesh, *ISRN Org. Chem.*, vol. 12, pp. 12, 2013.
- [59] K. N. Green, H. M. Johnston, M. E. Burnett, S. M. Brewer, *Comments. on Inorg. Chem.*, vol. 37, pp.146, 2016.
- [60] P. Gans, A. Sabatini, A. Vacca, *Talanta*, vol. 43, pp. 1739, 1996.
- [61] L. Zekany, I. Nagypal, G. Peintler, *PSEQUAD Version 5.01*, 2001.
- [62] M. A. Santos, S. M. Marques, S. Chaves, *Coord. Chem. Rev.*, vol. 256, pp. 240, 2012.
- [63] E. T. Clarke, A. E. Martell, *Inorg. Chim. Acta.191*, vol. 191, pp. 57, 1992

- [64] Z. D. Liu, R. C. Hider, *Coord. Chem. Rev.*, vol. 232, pp. 151, 2002.
- [65] E. V. M. Nurchi, G. Crisponi, T. Pivetta, M. Donatoni, M. Remelli, *J. Inorg. Bio. chem.*, vol. 102, pp. 684, 2008.
- [66] W. L. F. Armarego, D. D. Perrin, *Purification of Laboratory Chemicals*, 4th ed., Butterworth-Heinemann, Oxford, 1999.
- [67] W. Luo, Y. Ping-Li, Y. He, S. L. Huang, J. H. Tan, T. M. Ou, D. Li, L. Q. Gu, Z. S. Huang, *Bioorg. & Med. Chem.*, vol. 19, pp. 763, 2011.
- [68] S. Birman, *J. Bio. chem.*, vol. 225, pp. 825, 1985.
- [69] J. Sebestik, S. M. Marques, P. L. Fale, S. Santos, D. M. Arduino, S. M. Cardoso, C. R. Oliveira, M. L. Serralheiro, M. A. Santos, *Enzyme Inhib. Med. Chem.*, vol. 26, pp. 485, 2011.
- [70] M. Bartolini, C. Bertucci, M. L. Bolognesi, A. cavalla, C. Melchiorre, V. Andrisano, *Chem. Bio. Chem.*, vol. 8, pp. 2152, 2007.
- [71] F. J. C. Rossotti, H. Rossotti, *J. Chem. Educ.*, vol. 42, pp. 375, 1965.
- [72] R. M. Smith, A. E. Martell, *critical stability constant*, vol. 4, Plenum Press, New York, 1976.
- [73] T. Hassinen, M. Perakyla, *J. Comput. Chem.*, vol. 22, pp. 1229, 2001.

Appendix

Annexure 1.

The free radical scavenging of the compounds in the solution was calculated as percentage (%) of DPPH decoloration using the equation

$$I (\%) = (A_{\text{blank}} - A_{\text{sample}} / A_{\text{blank}}) \times 100$$

Where A_{blank} is the absorbance of the control reaction mixture excluding the test compounds, and A_{sample} is the absorbance of the test compound. Then this percentage I (%) is plotted against the concentration of compound under investigation, from there radicals scavenging potential as EC_{50} was calculated, which represents the sample concentration at which 50% of the DPPH radicals were scavenged by the concentration of compound and expressed in μM .

The inhibition curves were obtained by plotting the percentage of radical scavenging vs. inhibitor concentration and a calibration curve was drawn from which the linear regression parameters were obtained. The final values were obtained as the mean of two different experiments.

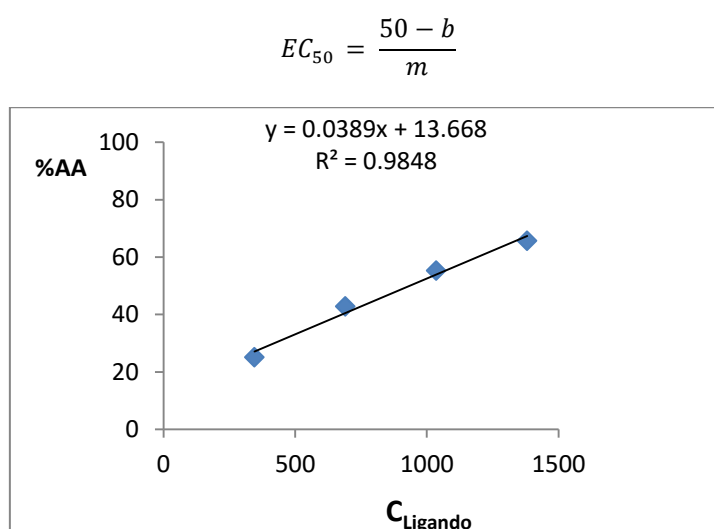


Figure 9. Graph for the calculation of % absorbance of ligand (TACHP-9) as EC_{50} .

Annexure 2.

The velocities of the reaction were calculated as well as the enzyme activity. A control reaction was carried out using the methanol solvent in the absence of the testing compound and it was considered as 100% activity. The percentage inhibition of the enzyme activity due to the presence of increasing compound concentration is calculated by the following equation

$$\%I = 100 - (V_I / V_0 * 100)$$

in which V_I is the initial reaction rate in the presence of inhibitor, and V_0 is the initial rate of the control reaction. The inhibition curves were obtained by plotting the percentage of enzymatic inhibition vs. inhibitor concentration and a calibration curve was drawn from which the linear regression parameters were obtained. The final values were obtained as the mean of two different experiments.

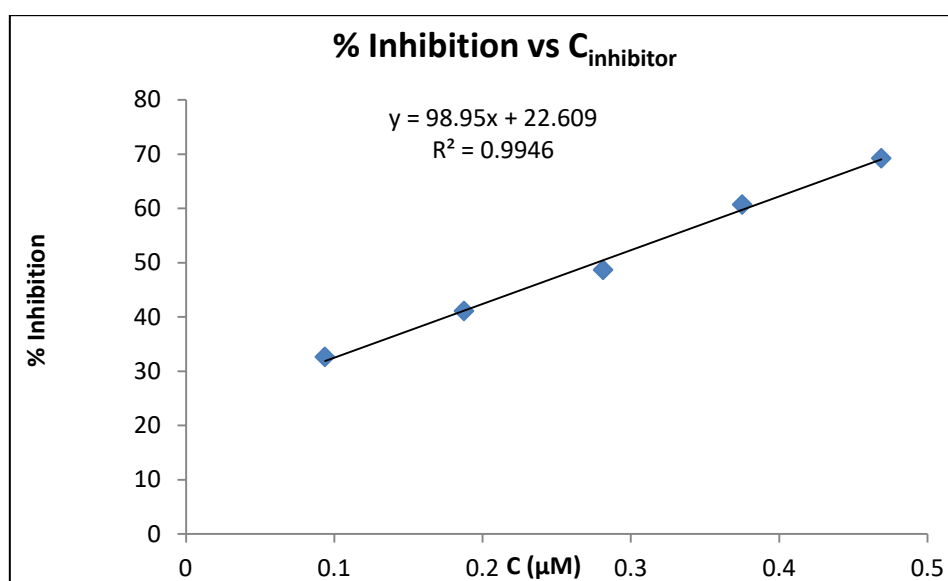


Figure 10. Graph for the calculation of AChE inhibition as IC_{50} by respective concentration of inhibitor (**RSC-6**).

$$IC_{50} = \frac{50-b}{m}$$

Where

$$m = 90.95$$

$$b = 22.60$$

$$IC_{50} = 0.27 \mu M.$$

Annexure 3.

The percent inhibition of the self-induced aggregation due to the presence of the test compound (**RSC-1**) was calculated on basis of equation

$$\%I = 100 - (IF_1/IF_0 * 100)$$

in which IF_1 and IF_0 correspond to the fluorescence intensities, in the presence and absence of the test compound (**RSC-1**), respectively, minus the fluorescence intensities due to the respective blanks. The reported values were obtained as the mean of two different experiments.